

## NMR-Solution Structures of Fluoro-Substituted $\beta$ -Peptides: A $3_{14}$ -Helix and a Hairpin Turn. The First Case of a $90^\circ$ O=C–C–F Dihedral Angle in an $\alpha$ -Fluoro-Amide Group

by Raveendra I. Mathad<sup>1)</sup>, Bernhard Jaun\*, Oliver Flögel<sup>2)</sup>, James Gardiner<sup>3)</sup>, Markus Löweneck<sup>4)</sup>, Jeroen D. C. Codée<sup>5)</sup>, Peter H. Seeberger, and Dieter Seebach\*

Laboratorium für Organische Chemie, Departement Chemie und Angewandte Biowissenschaften, ETH-Zürich, HCI Hönggerberg, Wolfgang-Pauli-Strasse 10, CH-8093 Zürich

and

Michael K. Edmonds, Florian H. M. Graichen, and Andrew D. Abell<sup>6)</sup>

Department of Chemistry, University of Canterbury, Private Bag 4800, Christchurch, New Zealand

Dedicated to Prof. Dr. Miguel Yus on the occasion of his 60th birthday

To further study the preference of the *antiperiplanar* (*ap*) conformation in  $\alpha$ -fluoro-amide groups, two  $\beta$ -peptides, **1** and **2**, containing a (2-F)- $\beta^3$ hAla and a (2-F)- $\beta^2$ hPhe residue, have been synthesized. Their NMR-solution structures in CD<sub>3</sub>OH were determined and compared with those of non-F-substituted analogs, **3** and **4a**. While we have found in a previous investigation (*Helv. Chim. Acta* **2005**, *88*, 266) that a stereospecifically introduced F-substituent in the central position of a  $\beta$ -heptapeptide is capable of 'breaking' the  $3_{14}$ -helical structure by enforcing the F–C–C=O *ap*-conformation, we could now demonstrate that the same procedure leads to a structure with the unfavorable *ca.*  $90^\circ$  F–C–C=O dihedral angle, enforced by the  $3_{14}$ -helical folding in a  $\beta$ -tridecapeptide (*cf.* **1**; *Fig. 4*). This is interpreted as a consequence of cooperative folding in the longer  $\beta$ -peptide. A F-substituent placed in the turn section of a  $\beta$ -peptidic hairpin turn was shown to be in an *ap*-arrangement with respect to the neighboring C=O bond (*cf.* **2**; *Fig. 7*). Analysis of the non-F-substituted  $\beta$ -tetrapeptides (with helix-preventing configurations of the two central  $\beta^2/\beta^3$ -amino acid residues) provides unusually tight hairpin structural clusters (*cf.* **3** and **4a**; *Figs. 8* and *9*). The skeleton of the  $\beta$ -tetrapeptide H-(*R*)- $\beta^2$ hVal-(*R*)- $\beta^2$ hVal-(*R*)- $\beta^3$ hAla-(*S*)- $\beta^3$ hPhe-OH (**4a**) is proposed as a novel, very simple backbone structure for mimicking  $\alpha$ -peptidic hairpin turns.

**1. Introduction.** – *The Conformation of  $\alpha$ -Fluoro Amides.* In a  $\beta$ -peptidic  $3_{14}$ -helix, there is a lateral and an axial position at each tetrahedral C-atom in the folded chain.

- 1) Part of the Ph.D. Thesis of R. I. M., ETH Dissertation No. 17209.
- 2) Postdoctoral Research Fellow at ETH-Zürich, 2004–2006, financed by the *Deutsche Forschungsgemeinschaft*, by the *Swiss National Science Foundation*, Project No. 200020-100182, and by *Novartis Pharma AG*, Basel.
- 3) Postdoctoral Research Fellow at ETH-Zürich, 2004–2007, financed by the *New Zealand Foundation for Research Science and Technology*, Project No. SWSS0401.
- 4) Postdoctoral Research Fellow at ETH-Zürich, financed by the *Swiss National Science Foundation*, Project No. 200020-109065/1.
- 5) Postdoctoral Fellow in the group of Prof. P. H. Seeberger, ETH-Zürich 2005–2006.
- 6) Current address, School of Chemistry & Physics, University of Adelaide, SA 5005, Australia.

Since the pitch of the helix is *ca.* 4.8 Å, non-H-atom substituents cannot occupy the axial positions (*Fig. 1*) [1][2].

In a quest for non-H-atoms that might be accommodated in an axial position of the  $3_{14}$ -helix, we have previously prepared the enantiomerically pure diastereoisomers of various 3-amino-2-hydroxy and 3-amino-2-fluoro acids and incorporated them into  $\beta$ -peptides **A** (*Table 1*) [4]7).

To our surprise, a single F-atom was not only *allowed* to occupy an axial position (*Table 1*: Y = F in **A**, X = H,  $n = 3$ ,  $m = 1$ ; see also *Fig. 1*), it *had to be* in that position in

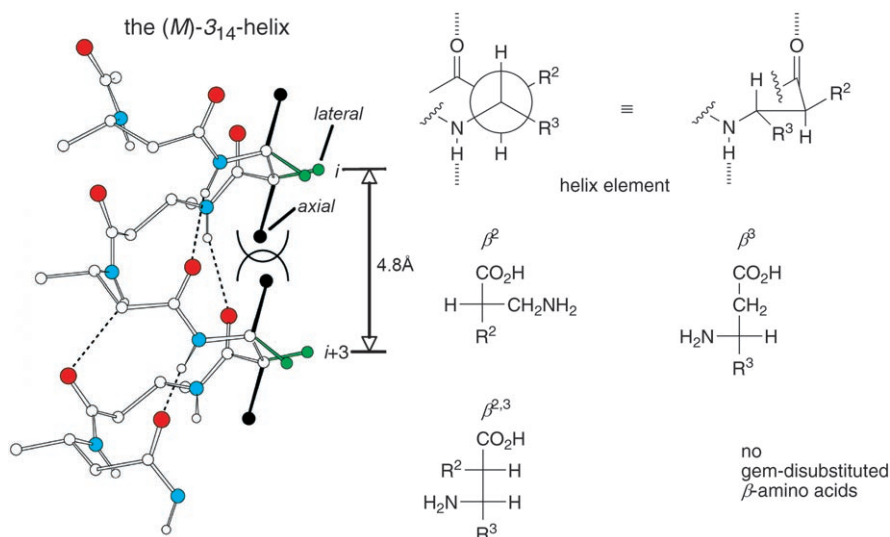


*Fig. 1.* The (*M*)- $3_{14}$ -helix with 'allowed' (blue) and 'forbidden' (black) positions for substituents  $R^2$  and  $R^3$  in the 2- and 3-position of each  $\beta$ hXaa residue. The  $\beta^2$ -,  $\beta^3$ -, and  $\beta^{2,3}$ -amino acids, which can be incorporated in a peptide folding to the (*M*)- $3_{14}$ -helix, are shown. A pitch of the helix may comprise more than exactly three residues, as seen in the NMR-solution structure of a  $\beta^3$ -icosamer [3].

*Table 1.* Various Types of  $\beta$ -Peptides Containing, or Consisting of F- and OH-Substituted  $\beta$ -Amino Acid Residues. R Groups are the side chains of Val, Ala, or Leu. X in lateral, Y in axial position of an (*M*)- $3_{14}$ -helix.

	$\text{H} \left[ \begin{array}{c} \text{R} \\   \\ \text{N} \\   \\ \text{H} \end{array} \right]_n \text{C}(\text{O}) \left[ \begin{array}{c} \text{R} \\   \\ \text{N} \\   \\ \text{H} \end{array} \right]_m \text{C}(\text{O}) \left[ \begin{array}{c} \text{R} \\   \\ \text{N} \\   \\ \text{H} \end{array} \right]_n \text{C}(\text{O})\text{OH} \quad \mathbf{A}$								
X	F	H	F	H	F	OH	H	H	F
Y	H	F	F	F	F	H	OH	OH	F
$n$	3	3	3	0	0	3	3	0	6
$m$	1	1	1	6	6	1	1	6	1

7) Proteinogenic  $\alpha$ -amino acid-derived *N,N*-dibenzylamino aldehydes [5] were the starting materials in our preparation [4b][4c]. For a route originating from 2-amino-3-hydroxy-acid esters, see [6].

order for a  $\beta$ -heptapeptide to adopt a  $3_{14}$ -helical secondary structure in MeOH solution (NMR analysis [4d]). The epimer ( $X = F$  in **A**,  $n = 3$ ,  $m = 1$ ,  $Y = H$ ) did not fold to a  $3_{14}$ -helix on the NMR time scale. Thus, a single ‘little fluorine’ placed stereospecifically in the middle of a  $\beta^3$ -heptapeptide was shown by this method to be able to ‘destroy’ the helix. Obviously, the well-known preference, according to theoretical calculations 6–8 kcal/mol [4d][7], of a C–F bond in an  $\alpha$ -fluoro amide for being *antiperiplanar* (*ap*) to the C=O bond is a strong enough effect to enforce a conformation of the (2*S*,3*S*)-3-amino-2-fluorobutanoic acid moiety (Table 1:  $Y = F$  in **A**,  $X = H$ ,  $n = 3$ ,  $m = 1$ ), which causes a bend in the backbone; in the (2*R*,3*S*)-epimer, the C–F bond is in the favorable *ap*-disposition with the C=O bond occupying an axial position in the  $3_{14}$ -helix. The degree to which the *ap* conformation is stabilized is evident from the result of a search in the *Cambridge Structural Database*, shown in Fig. 2.

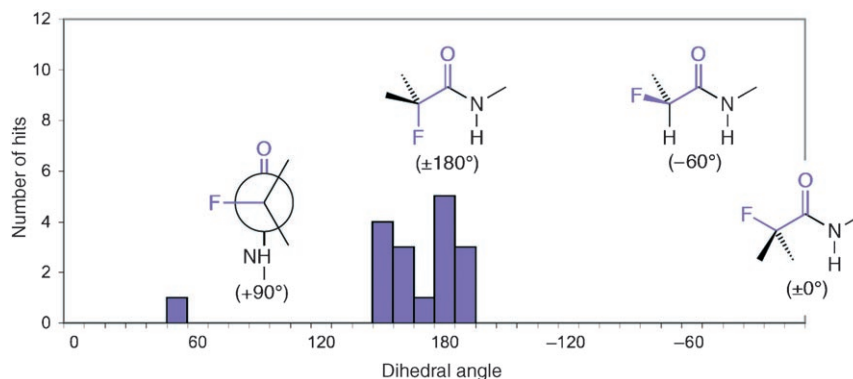
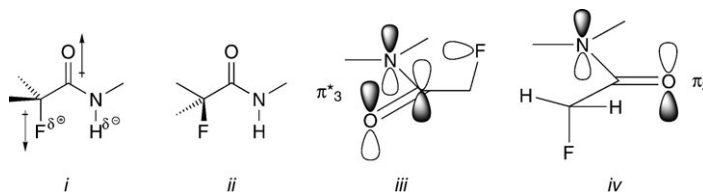


Fig. 2.  $F-C-C=O$  Dihedral angles in X-ray structures of  $\alpha$ -fluoro amides (only open chain structures were included); Cambridge Crystallographic Database Search as of August 1, 2007. At the date of search, there were also seven ‘hits’ of cyclic  $\alpha$ -fluoro amide structures with torsion angles of  $13$ ,  $24$ , and  $155 \pm 5^\circ$ .

The first reported structure of this type dates back to 1962 [8], with recent systematic investigations having been published by *O’Hagan* and co-workers [7][9]. For other  $\alpha$ -fluoro carbonyl compounds, such as *N,N*-dialkyl- $\alpha$ -fluoro amides,  $\alpha$ -fluoro esters, or  $\alpha$ -fluoro ketones, *synclinal* (*sc*,  $< 90^\circ$ , *gauche*), *anticlinal* (*ac*,  $> 90^\circ$ ,  $< 180^\circ$ ), and *synperiplanar* (*sp*,  $\pm 0^\circ$ ) dihedral  $F-C-C=O$  angles have also been reported [10–12]<sup>8)9)</sup>.

<sup>8)</sup> See the discussion of the preferred conformation of 2-F-, 2-Cl-, 2-Br-, and 2-I-cyclohexanone in [13].

<sup>9)</sup> According to IR measurements and MP2/6-31 + G (d,p) calculations, an *N*-methyl group ‘forces’ the C–F bond out of the amide plane (*cf. i, ii*) [12]. In the resulting conformation *iii* an  $n(F) \rightarrow \pi^*(\text{amide})$  interaction has been invoked [12]. A  $\pi(\text{amide}) \rightarrow \sigma^*(C-F)$  interaction, on the other hand, is not expected to stabilize such a conformation as the  $\pi_2$  amide orbital has a nodal plane through the carbon to which C–F is attached (*iv*).



There is, so far, no qualitative model that would rationalize the pronounced stability of the *ap*-conformation of  $\alpha$ -fluoro amides of the type shown in *Fig. 2*. Interactions between the coplanar C–F and N–H bonds (a kind of H-bonding), is suggested by the calculations [4d][7]. In ethane moieties ( $sp^3/sp^3$  bonds), the conformation with the C–F bond *ap* to a second polar C–X bond is less stable than that in which the two polar bonds are *sc* (*gauche*), an effect that can be regarded as resulting from a  $\sigma \rightarrow \sigma^*(C-F)$  interaction [14]. Simple dipole minimalization in the case of the fluoro amides, which is clearly not the dominating effect in F–CH<sub>2</sub>–CH<sub>2</sub>–X molecules, would appear to be especially important in the gas phase (*cf.* theoretical calculations, and *i* in *Footnote 9*), in non-polar solvents, and possibly also in crystal structures. Our NMR structures were, however, determined in MeOH, a rather polar, protic solvent.

**2. The Project: F-Substituted  $\beta$ -Peptidic Helix and Turn.** – To gain further experimental evidence for the *ap*-conformational preference of  $\alpha$ -fluoroamides, we have now synthesized new  $\beta$ -peptides containing 3-amino-2-fluoro acids.

One *target* molecule was the  $\beta$ -tridecapeptide **1** (*Fig. 3*), a  $\beta$ -peptide containing a central fluorobutanoic acid moiety of (2*S*,3*S*)-configuration previously known to have prevented helix-folding in the corresponding  $\beta$ -heptapeptide **A**,  $n = 3$ . In the longer  $\beta$ -peptide **1**, we could be sure [1] that the six  $\beta$ -amino-acid residues flanking the fluoro-amino acid moiety on each side would fold to a  $3_{14}$ -helix, and we were prepared to see an NMR-solution structure resembling the tendril of a pumpkin plant<sup>10)</sup> as shown in *Fig. 3*. In the N-terminal part of  $\beta$ -peptide **1**, the residues 3 ( $\beta^3$ hGlu) and 6 ( $\beta^3$ hLys) are positioned such that a salt-bridge interaction could act as a helix-stabilizing element [16–18]<sup>11)</sup>.

A *second target* was the *F*-substituted  $\beta$ -tetrapeptide **2**, and, for comparison, the non-fluorinated analog **3**, to investigate the  $\alpha$ -fluoro amide effect in a *hairpin-turn* structure. The choice of the particular turn elements in **2** and **3** calls for some comments: to date, we have constructed NMR-detectable  $\beta$ -peptidic turns only with longer peptides consisting of six [19] or eight [20]  $\beta$ -amino acid residues, the turn sections of which always contain an (*S*)- $\beta^2$ - and an (*S*)- $\beta^3$ -amino acid residue to form the ten-membered H-bonded ring **B**, and the (2*R*,3*S*)-3-amino-2-methyl acid building blocks giving rise to the antiparallel sheet section.

Everything else in the structure being equal, the use of two (*R*)- $\beta$ -amino acid residues as turn elements (*cf.* **3**) will lead to a reversed turn structure **C**, where the amide bond ‘flips’ *ca.* 180° just like when we go from a so-called  $\beta$ I- to a  $\beta$ I'- or to a  $\beta$ II-turn in the world of  $\alpha$ -peptidic turns [21][22]. In the present investigation, we *had* to use the (*R,R*)-configurational turn element for the simple reason that we only had the (*S*)-(2-fluoro)- $\beta^2$ hPhe derivative **5** at our disposal, which had been prepared as outlined in the *Scheme* [23]. A turn structure **D** with this F-substituted  $\beta^2$ -amino acid moiety was expected to profit from the  $\alpha$ -fluoro amide conformational effect discussed in the *Introduction*. There is another aspect to the use of two (*R*)-residues in a  $\beta$ -peptidic turn; while a  $\beta$ -peptide **4b** can ‘fall’ into the conformational manifold of  $3_{14}$ - or *12/10*-helical

<sup>10)</sup> For other examples of helices in the kingdom of plants, see [15].

<sup>11)</sup> We thank *F. Gessier* [4b][4c] for the sample of 3-amino-2-fluorobutanoic acid, which was used for the synthesis of **1**.

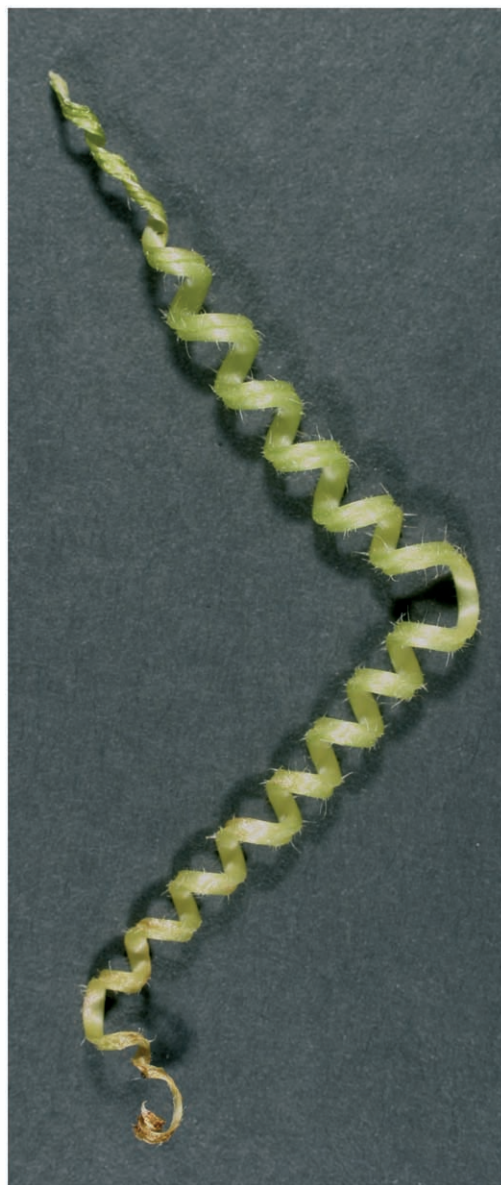
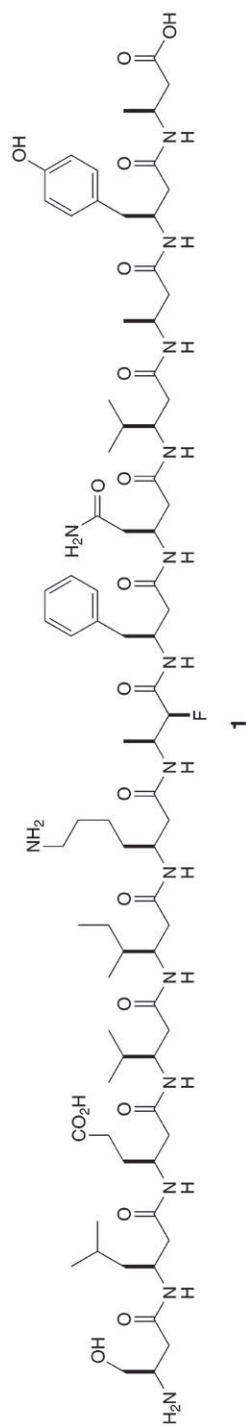
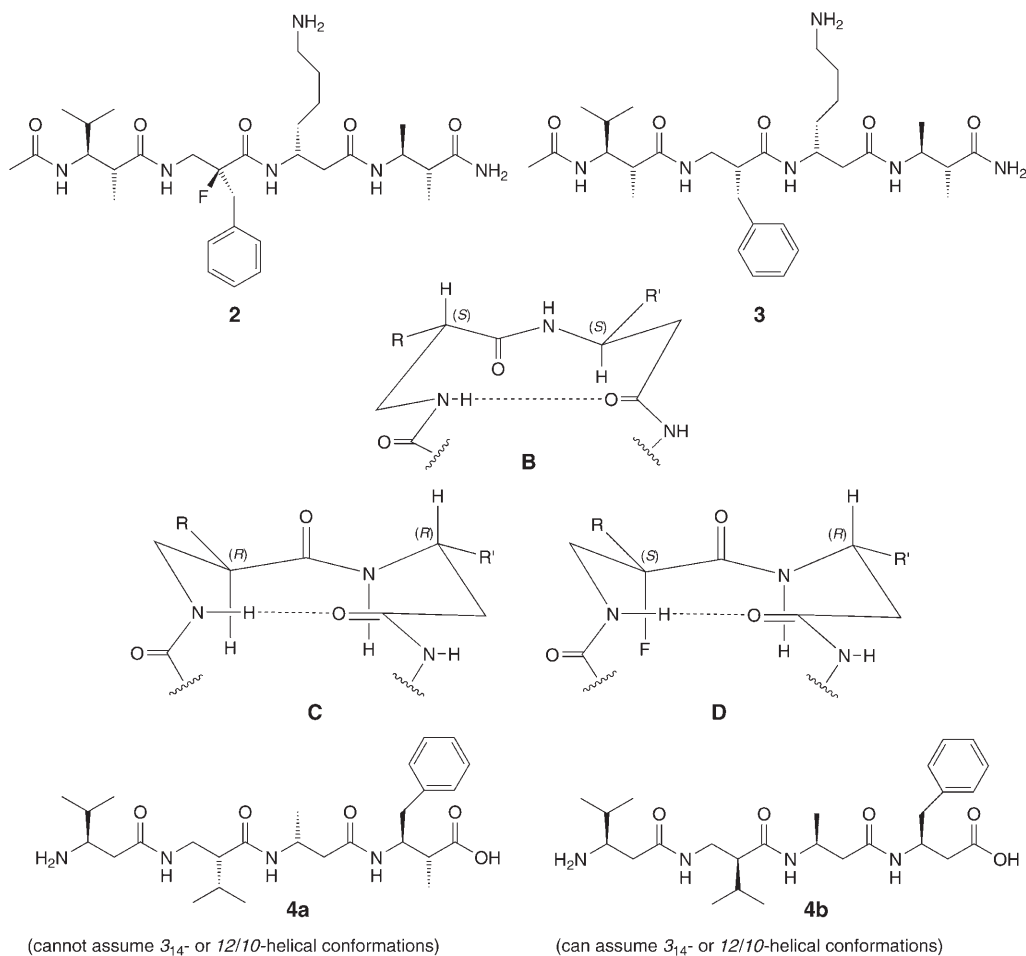
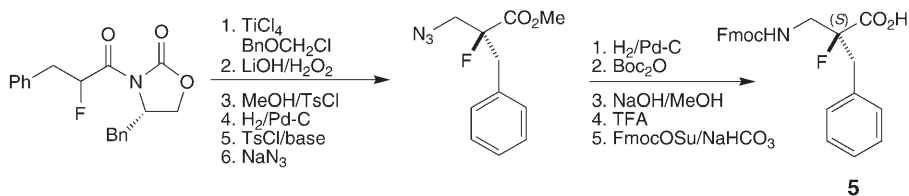


Fig. 3. Constitutional and configurational formula of  $\beta$ -tridecapeptide **1**. A tendril of a pumpkin plant containing a ca. 90° bend. Note that the helicity is (*P*) on the left and (*M*) on the right side of the bend (copyright R. Häffliger, ETH-Zürich).

(cannot assume  $3_{1,4}$ - or  $12/10$ -helical conformations)(can assume  $3_{1,4}$ - or  $12/10$ -helical conformations)

Scheme. Preparation of *Fmoc*-(*S*)-2*F*- $\beta^2$ *hPhe*-OH with an Evans Oxazolidinone Auxiliary. Bn = Benzyl; Ts = (4-methylphenyl)sulfonyl; Boc = *t*-BuOCO; TFA = CF<sub>3</sub>CO<sub>2</sub>H; *Fmoc* = [(9*H*-fluoren-9-yl)methoxy]-carbonyl; Su = *N*-succinimidoyl.



structures, the sequence **4a** cannot [1][19][20]. We, therefore, also investigated the NMR structure of the previously prepared  $\beta$ -tetrapeptide **4a** [24] for a comparative NMR-structural investigation.

The synthesis of the  $\beta$ -peptides **1–3** was achieved by solid-phase coupling on *Rink* amide resin, as described in the *Exper. Part*.  $\beta$ -Peptide **4a** was prepared *via* couplings in a microreactor [24]. The required 3-amino-2-methyl acids were at our disposal from previous work in the group [19b][20][25], and (*R*)-Fmoc- $\beta^2$ hPhe-OH, as well as (*R*)-Fmoc- $\beta^3$ hLys(Boc)-OH were obtained as described for the (*S*)-forms [25b][26][27].

### 3. NMR-Solution Structures and CD Spectra in MeOH of the F-Substituted $\beta$ -Peptides **1** and **2**, of the Non-F-Substituted Analog **3**, and of the $\beta$ -Tetrapeptide **4a**. –

3.1. *The  $\beta$ -Tridecapeptide 1*. The NMR spectrum of **1** in CD<sub>3</sub>OH showed good dispersion of signals allowing the complete assignment of all the <sup>1</sup>H-NMR resonances (Table 2).

Table 2. <sup>1</sup>H-NMR-Chemical Shifts of  $\beta$ -Tridecapeptide **1** in CD<sub>3</sub>OH

$\beta$ -Amino acid	NH ( <sup>4</sup> J(F <sub><i>i</i>-1</sub> ,HN))	CH <sub>2</sub> ( $\alpha$ )	H–C( $\beta$ ) ( <sup>3</sup> J(HN,H $\beta$ )/ <sup>3</sup> J(F $\alpha$ ,H $\beta$ ))	H–C( $\gamma$ )/ Me–C( $\gamma$ )/ CH <sub>2</sub> ( $\gamma$ )	H–C( $\delta$ )/ Me–C( $\delta$ )	Me–C( $\epsilon$ )
$\beta$ hSer <sup>1</sup>		2.59/3.06	3.71	3.83		
$\beta$ hLeu <sup>2</sup>	8.36	2.48/2.85	4.64 (9.46)	1.34, 1.53	1.63	0.95
$\beta$ hGlu <sup>3</sup>	8.55	2.36/2.48	4.34 (9.10)	1.87		
$\beta$ hVal <sup>4</sup>	8.39	2.43/2.72	4.32 (9.10)	1.8	0.96	
$\beta$ hIle <sup>5</sup>	7.92	2.61	4.28 (9.32)	1.6	1.0	
$\beta$ hLys <sup>6</sup>	8.13	2.53/2.83	4.46 (9.32)	1.63	1.44	1.65
$\beta$ hAla( $\alpha$ F) <sup>7</sup>	8.69	5.10	4.57 (9.68, 12.0)	1.24		
$\beta$ hPhe <sup>8</sup>	8.78 (< 1.0)	2.33/2.63	4.63 (9.10)			
$\beta$ hAsn <sup>9</sup>	8.41	2.44/2.51	4.80 (9.12)	2.63, 2.77		
$\beta$ hVal <sup>10</sup>	7.95	2.43/2.73	4.30 (9.40)	1.74	0.92	
$\beta$ hAla <sup>11</sup>	7.56	2.34	4.41 (8.95)	1.17		
$\beta$ hTyr <sup>12</sup>	7.73	2.29/2.59	4.57 (9.54)	2.61, 2.79		
$\beta$ hAla <sup>13</sup>	7.85	2.52	4.40 (8.50)	1.13		

The individual amino-acid spin systems were assigned by using a combination of DQF-COSY and TOCSY experiments. HSQC-HMBC Techniques were then used for sequential assignment. The <sup>3</sup>J(NH,H $\beta$ ) values were extracted from the 1-D <sup>1</sup>H-NMR spectrum, and large coupling constants established that NH and H $\beta$  are in *antiperiplanar* arrangement throughout the sequence. Qualitative inspection of ROESY revealed NOEs between the NH<sub>*i*</sub> proton and H $\beta$  of residues *i* + 2, *i* + 3 that are characteristic of the  $3_{14}$ -helical structure. A ROESY spectrum was acquired with  $\tau_m = 300$  ms and integration of the cross-peaks, followed by calibration with known distances, yielded inter-proton distances. The distances, together with dihedral angles around NH and H $\beta$ , as derived from the coupling constants, were used as constraints in MD-simulated annealing (SA) calculations according to the X-PLOR protocol. This calculation yielded a set of 30 structures with low violations; they are shown in Fig. 4. The side chains of the individual conformers superimpose fairly tightly, suggesting that this  $\beta$ -tridecapeptide adopts a well-defined structure in CD<sub>3</sub>OH solution. The bundle shows a  $3_{14}$ -helix over the full length of the sequence and, as a consequence, the F-atom occupies a *lateral* position on the helix! The C–F bond is not *anti* but rather at an

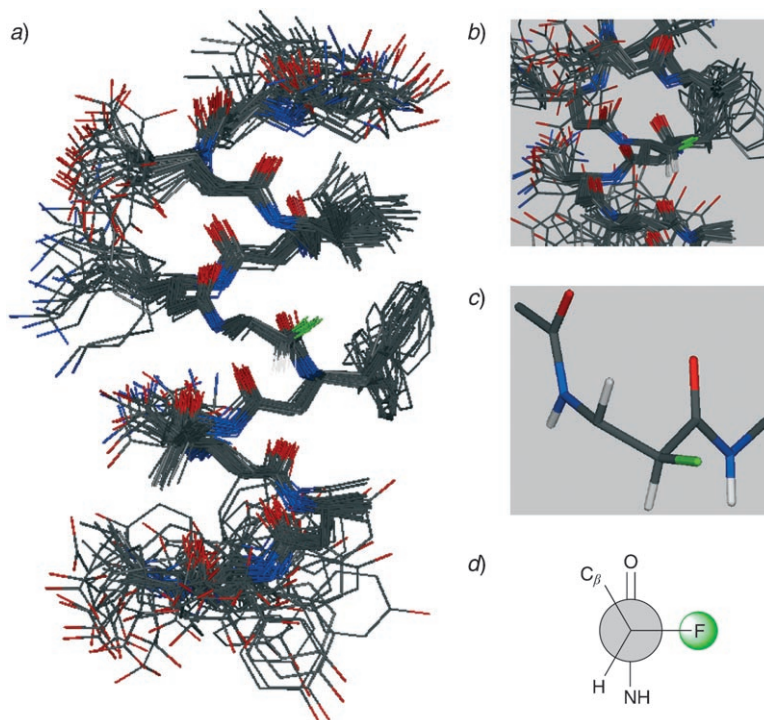


Fig. 4. The  $^3_1$ -helical NMR structure of the tridecapeptide **1** in  $CD_3OH$ . a) Overlay of 20 of the 30 lowest-energy structures obtained by SA calculation. For the fit of backbone atoms (N, C( $\alpha$ ), C( $\beta$ ), and C), the MOLMOL [28] program was used. b) and c) Zooming-in on the F-substituted amino acid residue **4** in the central position of  $\beta$ -tridecapeptide **1**. d) Newman projection along the F–C–C=O bond in **1**.

almost  $90^\circ$  angle with respect to the amide plane, a local conformation which must be considered unfavorable based on both the theoretical calculations and the experimentally determined structures of  $\alpha$ -fluoroamides discussed in *Chapt. 1*<sup>12</sup>).

<sup>12</sup>) A detailed 2D-NMR-spectroscopic analysis was also undertaken to obtain conformational information on peptides **A** ( $n=0$ ,  $m=6$ , X=H, Y=F) in  $CD_3OH$  and **A** ( $n=0$ ,  $m=6$ , X=Y=F) in DMSO. The complete assignment of all  $^1H$ -NMR resonances and the sequential assignment were achieved by using the standard procedure. To study the preferred conformations of the poly-heteroatom substituted backbones of these  $\beta$ -peptides, the use of  $^3J(H,F)$  or  $^3J(C,F)$  coupling constants would be useful, in order to gain more specific information on dihedral angles. Although the use of  $^3J(H,H)$  couplings in conformational analysis is well-established, this is not yet the case for  $^3J(H,F)$  or  $^3J(C,F)$  because the corresponding *Karplus* coefficients are strongly dependent on the individual substituents on the two C-atoms and are, as yet, uncalibrated for the case of  $\alpha$ -fluoro- $\beta^3$ -amino acid units. The distance constraints were derived from the ROESY spectrum measured with  $\tau_m = 300$  ms. Even though observation of the large  $^3J(NH,H\beta)$  and of NH–NH NOEs was initially indicative of a helical structure, only intra-residual and sequential NOEs were observed. Further SA annealing calculations with X-PLOR confirmed that the conformations of these two ‘perfluorinated’  $\beta$ -peptides are of non-helical nature in the solvents used for the NMR measurements. (*R. I. M.*, Dissertation referred to in *Footnote 1*).



The CD spectrum of the  $\beta$ -tridecapeptide **1** (Fig. 5) is compatible [1] with the  $3_{14}$ -helical structure as determined by NMR spectroscopy: there is a negative *Cotton* effect near 215 and a positive one near 200 nm.

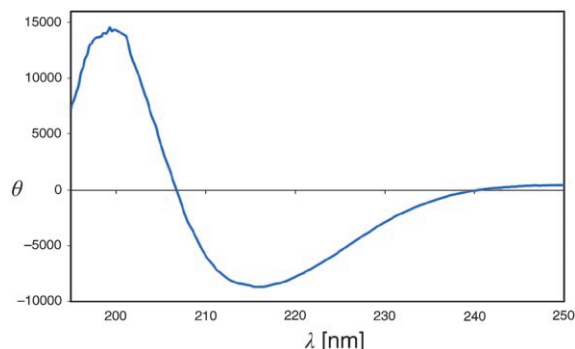


Fig. 5. Normalized CD spectrum of **1** in MeOH (0.2 mM)

3.2. The  $\beta$ -Tetrapeptides **2**, **3**, and **4a**. 3.2.1. CD Spectra. For turn structures containing the  $(S)\beta^2\text{hXaa}-(S)\beta^3\text{hXaa}$  element, we have observed [1][19][20] the same type of CD spectrum as for the  $\beta^2/\beta^3$ -10/12-helical structures [25b][29]: a single maximum near 205 nm (Fig. 6, a and b)<sup>13</sup>.

The CD spectra of the novel  $\beta$ -tetrapeptides **2** and **3** in MeOH are shown in Fig. 6, c and d. The non-F-substituted compound **3** gives rise to a mirror-image-type pattern (negative *Cotton* effect at 202 nm) as compared to that of ‘conventional’  $\beta$ -peptidic turns (cf. Fig. 6, a and b); the F-containing analog **2** has a CD spectrum (Fig. 6, c) with a minimum of somewhat lower intensity at 200 nm, and a broad, weaker positive *Cotton* effect near 222 nm. Thus, the sign of the short-wavelength *Cotton* effect is reversed from plus to minus when the turn section contains heterochiral  $\beta^2/\beta^3$ -amino acids (see the boxed parts of the *Formulae* in Fig. 6, and compare the representations **B** and **C** in *Chapt. 2* above), irrespective of the fact that the terminal amino-acid residues are homochiral.

The CD spectrum of compound **4a** in MeOH is shown in Fig. 6, e – a big surprise: there is a single, broad *maximum* at 210 nm! Although this  $\beta$ -tetrapeptide **4a** contains central  $(R)\beta^2-(R)\beta^3$  residues, just like peptide **3**, there is no resemblance between their CD spectra (compare Fig. 6, c, with Fig. 6, e). If both compounds **3** and **4a** would fold to the same kind of turn (see **C** in *Chapt. 2* above), and if the chirality of this turn would generate the *Cotton* effect, as discussed in the previous paragraph, we would expect a *minimum* near 200 nm in the CD spectrum of  $\beta$ -peptide **4a**. There are two structural differences between **3** and **4a**: the  $\beta$ -tetrapeptide **3** contains terminal disubstituted (sheet-inducing)  $\beta^{2,3}$ -amino acid residues and amide groups at both *termini*, while  $\beta$ -

<sup>13</sup>) To observe more or less identical spectra for such different species as a *turn* (consisting of a ten-membered H-bonded ring with attached *antiparallel* sheet section, built of 14-membered *trans*-catenate H-bonded rings) and a *(P)*-helix (consisting of alternating ten- and twelve-membered H-bonded rings) was not a promising aspect for obtaining structural information about  $\beta$ -peptides from CD spectroscopy! See our comments in [1] and in publications dedicated to this topic [30].

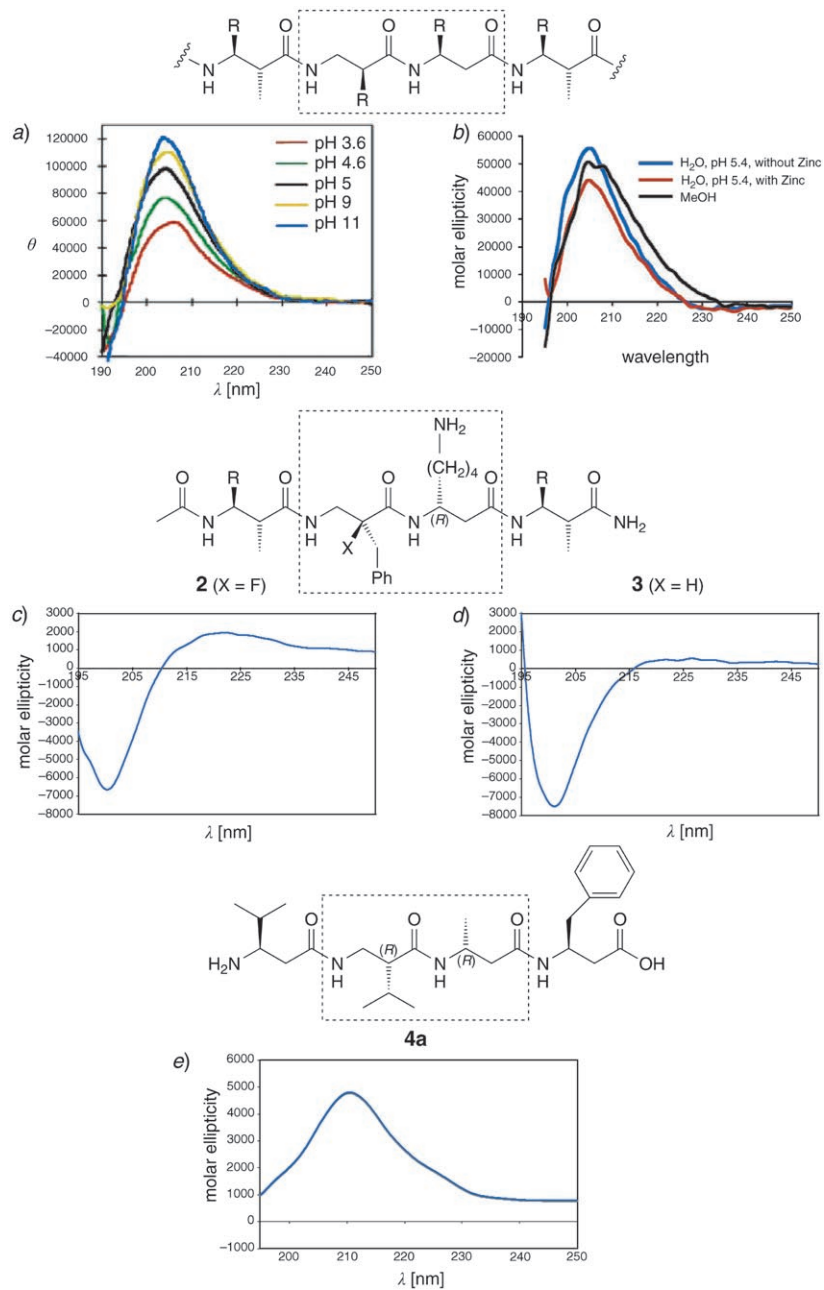


Fig. 6. CD Spectra of  $\beta$ -peptides forming a turn of type **B** (a and b, non-normalized), and of the novel  $\beta$ -peptides **2**, **3**, and **4a** (c, d, and e, respectively; normalized). The opposite sign of the Cotton effect near 200 nm in a and b as compared to c and d would be compatible with a 'mirror-image' structure of the turns (cf. **B** with **C/D** in *Chapt. 2*). A different structure is suggested by the CD spectrum of **4a** as shown in e. The curves shown in a and b are reproduced from [1][19b], and [20], resp.

tetrapeptide **4a** is missing these two structural features: **4a** contains ‘free’ termini, was not isolated as trifluoro-acetate salt, and may exist as a zwitterion.

Thus, we are left with yet another situation in which CD spectra of  $\beta$ -peptides are more puzzling than helpful.

Considering the uncertainty of  $\beta$ -peptidic CD patterns for obtaining reliable information<sup>13</sup>), the structures of the three peptides **2**, **3**, and **4a** had to be determined by NMR investigations.

3.2.2. *Solution Structures of  $\beta$ -Tetrapeptides 2, 3, and 4a.* All three compounds were subjected to a detailed NMR analysis in CD<sub>3</sub>OH. Sequence-specific assignments were achieved by using standard 2D-NMR techniques as described earlier in Sect. 3.1. The chemical shifts and coupling constants are compiled in Tables 3–5.

The large  $^3J(\text{HN}, \text{H}\beta)$  and  $^3J(\text{H}\beta, \text{H}\alpha)$  values (9.0–10 Hz) for the terminal residues clearly suggest that these residues adopt an extended structure. In peptides **2** and **3**, a value of ca. 9 Hz for  $^3J(\text{HN}, \text{H}\beta)$  in the  $\beta^3\text{hLys}$  residue forming one corner of the turn indicates that H $\beta$  and HN are also nearly antiperiplanar in this residue. In the  $\beta^2\text{hPhe}$  residue forming the other corner of the turn, however, neither of the two H $\beta$  protons are exactly antiperiplanar to the HN as indicated by  $^3J(\text{HN}, \text{H}\beta)$  values of 7.8 and 4.4 Hz. Therefore, this dihedral angle was not constrained in the structure calculations. ROESY Spectra with  $\tau = 300$  ms of peptides **2** and **3** were recorded to obtain distance constraints by integration of NOE cross-peaks using the two-spin approximation. The distances, together with dihedral angles, were used as constraints in MD-simulated annealing calculations by following the X-PLOR protocol. Each calculation yielded a set of 30 structures with low violations; they are shown in Fig. 7 for the fluorinated compound **2**, and in Fig. 8 for the non-fluorinated compound **3**.

Clearly, both peptides fold to a hairpin structure with a central turn unit, formed by the  $\beta^2/\beta^3$ -amino acid section, involved in a ten-membered H-bonded-ring. As expected, the orientation of the amide bonds is ‘reversed’, as compared to that of turns built of  $\beta^2/\beta^3$ -amino acids of opposite chirality (*cf.* **B** vs. **C** and **D** in Chapt. 2). In the case of the F-substituted  $\beta$ -tetrapeptide **2**, the SA calculations yielded two sets of conformers: in one (80% of the accepted structures), the F–C bond is oriented nearly *antiperiplanar* to the C=O bond, as expected for an  $\alpha$ -fluoro amide. In the second conformation (20% of the accepted structures), the dihedral angle F–C–C=O is between 140 and 160° which must be considered less favorable, as discussed in the *Introduction*. Qualitative analysis of the NOE pattern indicates that the calculated structures are largely determined by a set of NOEs between the amino acids in the two antiparallel terminal sections. For the region of the two amino acids in the turn, however, the structure is not so well-defined by the observable NOEs, in part because C( $\alpha$ ) of ( $\alpha$ F)- $\beta^2\text{hPhe}$  is doubly substituted and carries no proton. Since no reliable calibrations for the vicinal  $^3J(\text{H}, \text{F})$  coupling constants in  $\alpha$ -fluoro- $\beta^3$ -amino acid residues are available yet (see *Footnote 12*), we had to abstain from using corresponding constraints in the SA calculations, and this was the major cause for the appearance of two different conformational clusters in the bundle of accepted structures.

Qualitative information on the backbone dihedral angles can nevertheless be deduced from the H,F-coupling constants as follows. In  $\beta^3$ -peptides containing an axially oriented  $\alpha$ -F-substituent within a well-defined  $3_{14}$ -helical structure (*i.e.*, X=F, Y=H,  $m=3$ ,  $n=1$  in Table 1 [4d]), we observed a long-range coupling of ca. 4 Hz

Table 3.  $^1\text{H}$ - and  $^{13}\text{C}$ -NMR Chemical Shifts of the *F*-Substituted  $\beta$ -Tetrapeptide **2** in  $\text{CD}_3\text{OH}$ 

$\beta$ -Amino acid	NH ( $^4J(\text{F}_{-1}, \text{HN})$ )	$\text{CH}_2(\alpha)$	$\text{H}-\text{C}(\beta)$ ( $^3J(\text{HN}, \text{H}\beta)$ , $^3J(\text{F}\alpha, \text{H}\beta)$ )	$\text{H}-\text{C}(\gamma)/\text{Me}-\text{C}(\gamma)/\text{CH}_2(\gamma)$	$\text{H}-\text{C}(\delta)/\text{Me}-\text{C}(\delta)$	$\text{H}-\text{C}(\epsilon)/\text{Me}-\text{C}(\epsilon)$	$\text{C}(\alpha)$	$\text{C}(\beta)$	$\text{C}(\gamma)$	$\text{C}(\delta)$
$\beta^{2,3}\text{hVal}(\alpha\text{Me})^1$	7.65	2.71	4.13 (10.20)	1.80	0.88/0.92		44.33	57.34	31.30	16.90
$\beta^2\text{hPhe}^2$	8.34		3.55 (7.80, 22.6), 3.92 (4.40, 18.2)	3.10/3.20			99.98	48.55	43.86	
$\beta^3\text{hLys}^3$	7.82 (3.9)	2.22/2.32	4.04 (8.95)	1.21/1.30	0.79	1.45	40.83	48.39	34.43	28.34
$\beta^{2,3}\text{hAla}(\alpha\text{Me})^4$	7.89	2.42	4.03 (8.70)	1.12			47.90	48.84	15.41	

Table 4.  $^1\text{H}$ - and  $^{13}\text{C}$ -NMR Chemical Shifts of the Non-*F*-Substituted  $\beta$ -Tetrapeptide **3** in  $\text{CD}_3\text{OH}$ 

$\beta$ -Amino acid	NH	$\text{CH}_2(\alpha)$	$\text{H}-\text{C}(\beta)$ ( $^3J(\text{HN}, \text{H}\beta)$ )	$\text{H}-\text{C}(\gamma)/\text{Me}-\text{C}(\gamma)/\text{CH}_2(\gamma)$	$\text{H}-\text{C}(\delta)/\text{Me}-\text{C}(\delta)$	$\text{H}-\text{C}(\epsilon)/\text{Me}-\text{C}(\epsilon)$	$\text{C}(\alpha)$	$\text{C}(\beta)$	$\text{C}(\gamma)$	$\text{C}(\delta)$
$\beta^{2,3}\text{hVal}(\alpha\text{Me})^1$	7.66	2.61	4.11 (10.34)	1.79	0.88/0.99		44.26	57.53	31.36	16.84
$\beta^2\text{hPhe}(\alpha\text{F})^2$	8.32	2.74	3.31, 3.32	2.78			50.35	43.14	37.31	
$\beta^3\text{hLys}^3$	7.80	2.21/2.28	4.06 (8.80)	1.35	1.41/1.45	0.85	42.79	47.82	34.72	28.08
$\beta^{2,3}\text{hAla}(\alpha\text{Me})^4$	7.88	2.41	4.05 (8.88)	1.10			46.78	48.83	15.30	

Table 5.  $^1\text{H}$ - and  $^{13}\text{C}$ -NMR Chemical Shifts of  $\beta$ -Tetrapeptide **4a** in  $\text{CD}_3\text{OH}$ 

$\beta$ -Amino acid	NH	$\text{CH}_2(\alpha)$	$\text{H}-\text{C}(\beta)$ ( $^3J(\text{HN}, \text{H}\beta)$ )	$\text{H}-\text{C}(\gamma)/\text{Me}-\text{C}(\gamma)/\text{CH}_2(\gamma)$	$\text{H}-\text{C}(\delta)/\text{Me}-\text{C}(\delta)$	$\text{C}(\alpha)$	$\text{C}(\beta)$	$\text{C}(\gamma)$	$\text{C}(\delta)$
$\beta^{2,3}\text{hVal}(\alpha\text{Me})^1$		2.47, 2.65	3.35	1.92	0.99	36.42	55.75	31.87	20.25
$\beta^2\text{hVal}^2$	8.26	2.15	3.14, 3.56	1.79	0.89, 0.97	54.25		30.04	21.24
$\beta^3\text{hAla}^3$	7.81	2.16, 2.39	4.14 (8.07)	0.98		42.65		18.59	
$\beta^{2,3}\text{hPhe}(\alpha\text{Me})^4$	7.98	2.33	4.43 (8.75)			43.69	50.71	41.81	

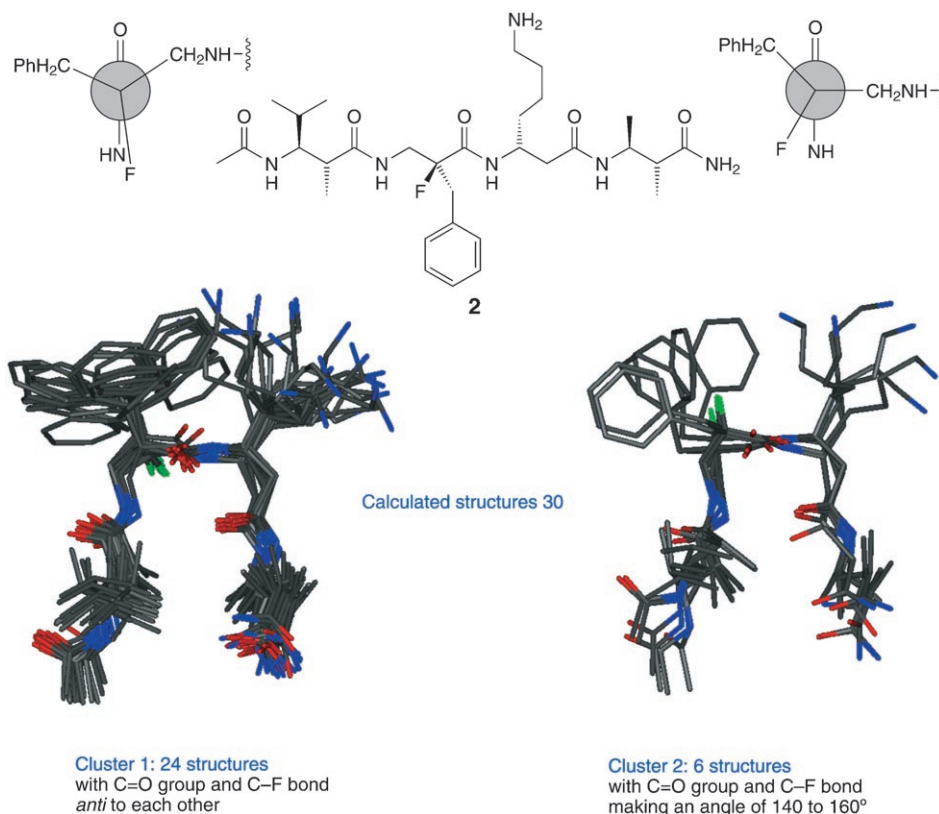


Fig. 7. Solution structure of  $\beta$ -tetrapeptide **2** in  $CD_3OH$ . Overlay of the 30 lowest energy structures obtained by SA calculation are shown. *a*) Cluster 1: A hairpin structure of  $\beta$ -peptide **2** showing C-F and C=O bonds in *antiperiplanar* arrangement with both  $CH_2Ph$  and  $(CH_2)_4-NH_2$  side chains occupying equatorial positions on the turn segment of the hairpin structure. *b*) Cluster 2: A distorted hairpin structure of  $\beta$ -peptide **2** showing C-F and C=O bonds moving away from the 'ideal' *antiperiplanar* conformation. This cluster can be rejected based on the observed  $^4J(F\alpha-HN_{i+1})$  coupling.

between the  $\alpha$ -F and the HN proton of the next amino acid in the sequence. In the  $\beta$ -peptide **1** discussed above, where the structure is helical but the F-C( $\alpha$ )-C=O dihedral angle is near  $90^\circ$ , this long-range coupling is absent ( $< 1$  Hz). Therefore, we interpret this  $^4J(F\alpha, HN_{i+1})$  coupling as an indicator of coplanarity of the F-C( $\alpha$ )-C-N-H fragment, *i.e.*, of a near *antiperiplanar* orientation of the F-C( $\alpha$ ) and C=O bonds. Because such a  $^4J(F\alpha, HN_{i+1})$  coupling of 4 Hz was observed for fluoro peptide **2**, the corresponding dihedral angle must be near  $180^\circ$  and the 2nd cluster found in the SA calculations based on NOEs, and other dihedral angle constraints alone can be rejected. Compared to the value of *ca.* 32 Hz observed for the  $^3J(H\beta, F\alpha)$  coupling in structures such as those referred to in Table 1 (*i.e.*, X = F, Y = H,  $m = 3$ ,  $n = 1$  [4d]) with a nearly perfect *antiperiplanar* arrangement of these nuclei, the corresponding values of *ca.* 23 Hz and 18 Hz observed for the ( $\alpha$ F)- $\beta^2$ hPhe residue in **2** indicate a deviation of the dihedral angle around the C( $\alpha$ )-C( $\beta$ ) bond from the ideal staggered conformation.

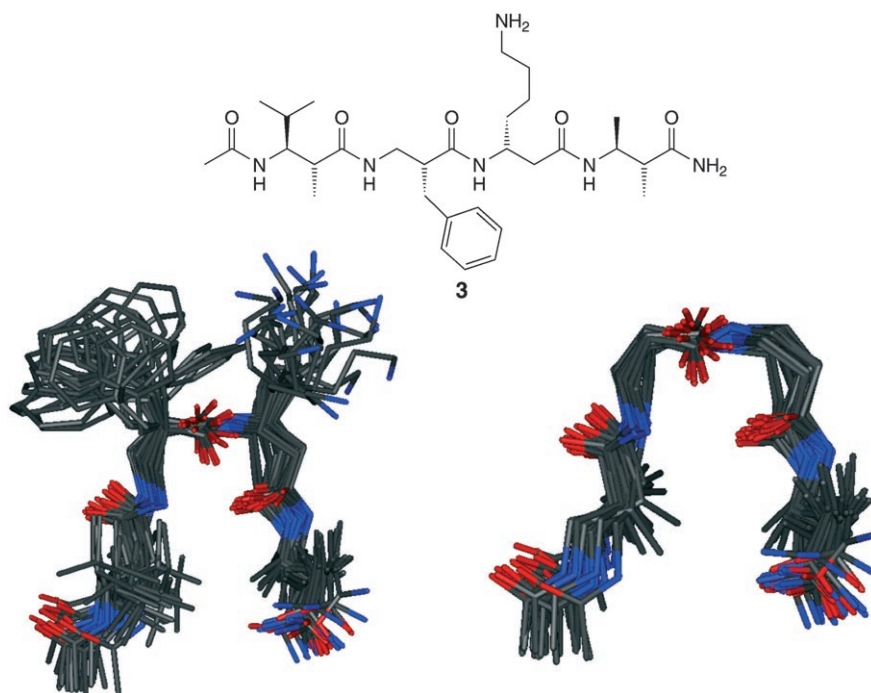


Fig. 8. NMR-Solution structure of  $\beta$ -tetrapeptide **3** in  $CD_3OH$ . A bundle of low-energy structures calculated with the simulated annealing protocol shows a  $\beta$ II-type hairpin-turn structure stabilized by a ten-membered intramolecular H-bonded ring.

In contrast to  $\beta$ -tetrapeptide **2**, the distance and dihedral angle constraints derived from NOEs and  $^3J(H,H)$  coupling constants for the non-fluorinated analog **3** defined the structure well enough to give a single conformation of the backbone in the SA-annealing calculations (Fig. 8).

Analysis of the NMR data of the  $\beta$ -tetrapeptide **4a** with the (*R*)- $\beta^2$ hVal-(*R*)- $\beta^3$ hAla turn unit leads to an especially tight and dense cluster of hairpin structures (Fig. 9). Compound **4a** is the simplest  $\beta$ -peptide folding to a hairpin.

As pointed out above, **4a** does not contain any 3-amino-2-methyl acid residues (sheet inducing), nor does it contain terminal amide groups (providing for a *trans*-catenate H-bond), and there does not seem to be an interaction between the N-terminal  $NH_2$  (or  $NH_3^+$ ) and the C-terminal  $CO_2H$  (or  $CO_2^-$ ) groups (leading to H-bonding or salt-bridge attraction). The reversed configuration of the two central  $\beta$ -amino acid moieties leads to the desired turn stabilization (precluding competition with helical conformations). Thus,  $\beta$ -peptides of this type could present a better scaffold for mimicking  $\alpha$ -peptidic turns than the previously used derivatives [31].

**4. Discussion and Conclusions.** – The helix of the  $\beta$ -tridecapeptide **1** contains a central (2*S*,3*S*)-3-amino-2-fluorobutanoic acid residue in the conformation with the F–C bond more or less perpendicular to the amide plane (Fig. 4), an arrangement that

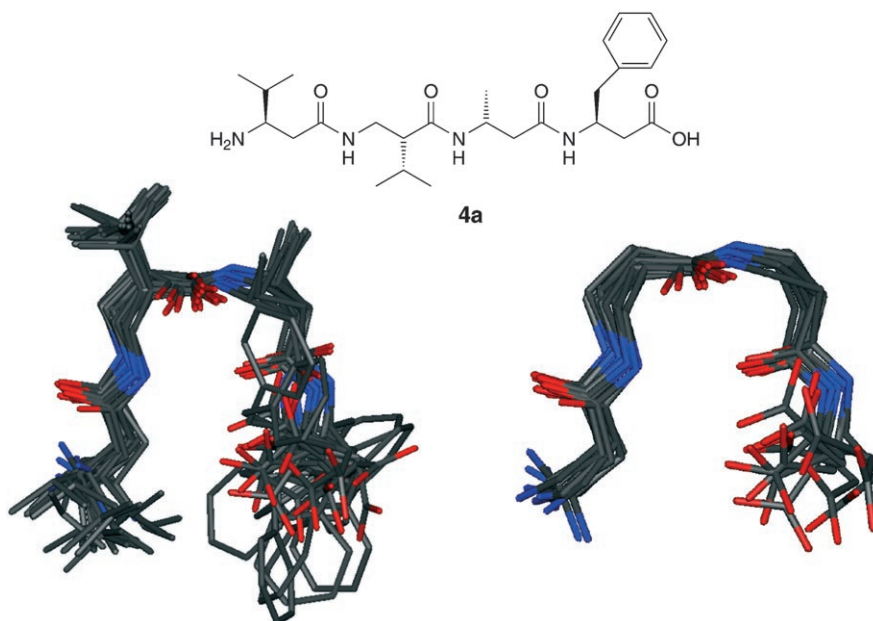


Fig. 9. NMR-Solution structure of  $\beta$ -tetrapeptide **4a** in  $CD_3OH$ . A set of low-energy hairpin structures obtained by SA calculations reveals a well-defined backbone, in spite of the fact that there are simple  $\beta^3$ -homoamino acid residues at both *termini*, and that there is only one H-bond!

is less stable by several kcal/mol than that in which the F–C bond is coplanar with the amide group and antiperiplanar with respect to the O=C bond. The conformation seen in this  $\beta$ -tridecapeptide structure is unprecedented in  $\alpha$ -fluoro amides. While the (2*S*,3*S*)-3-amino-2-fluoro acid residue in the centre of a  $\beta$ -heptapeptide is able to ‘break’ the helical structure [4d], this same amino acid residue is forced into an unstable conformation within the helical secondary structure of the  $\beta$ -tridecapeptide **1**. What provides the necessary enthalpy of supposedly [4d][7] 6–8 kcal/mol? A structure resembling the helix-bend-helix shape, as alluded to in Fig. 3, with two ‘independent’  $\beta$ -hexapeptide helices and the more stable *ap*-conformation of the fluoro-amino acid moiety in the centre, would have been more compatible with the results of our previous investigations of shorter  $\beta$ -peptides  $\leq 8$  residues long<sup>14</sup>). *i*) Only linear effects are seen in their CD and NMR spectra upon heating solutions up to 80° [33]; *ii*) the NMR spectrum of a helical  $\beta$ -peptide in MeOH changes linearly upon dilution with H<sub>2</sub>O [34]; *iii*) molecular-dynamics simulations [35] at elevated ‘*in silico*’ temperatures do not indicate sudden structural changes in  $\beta$ -peptidic helices. These results point to a non-cooperative folding of the  $3_{14}$ -helix, as sigmoidal dependences would have been observed otherwise. The interpretation of this behavior is that the enthalpic contributions (H-bonds, local preference for *gauche*-conformation of the C( $\alpha$ )-C( $\beta$ ) bonds, and side-chain stacking) within each turn are additive along the helix. If, on the

<sup>14</sup>) ... and also of  $\gamma$ -hexapeptides [32].

other hand, formation of a helical turn would favor the folding in adjacent turns, cooperative effects and a two-state ‘melting’ behavior would have to be observed. In the framework of this interpretation, the fact that  $\beta$ -tridecapeptide **1** is longer and can form extended helical regions on both sides of the F-substituted residue does not explain why the latter should be forced into a stereoelectronically unfavorable local conformation fitting into a  $3_{14}$ -helical structure. The reason for this must be in favorable interactions that extend beyond a single turn within the *tridecamer*, but which are absent in the shorter *heptapeptide*. Hints to such cooperative folding in longer  $\beta$ -peptides come from the fact that in a  $\beta^3$ -pentadecapeptide, the central NH groups underwent H/D exchange only very slowly in CD<sub>3</sub>OD (half-lives of up to 60 days [25b]). Furthermore, the recent investigation of  $\beta$ -peptidic quaternary structures (*cf.* a bundle of eight  $\beta^3$ -dodecamers) by Schepartz and co-workers [18][36] has demonstrated cooperative folding.

The  $\alpha$ -fluoro- $\beta$ -tetrapeptide **2** and its non-fluorinated analogue **3** essentially show the same solution structure, although the scarcity of NOEs in the region of the turn makes the structure of **2** somewhat less well defined, with reduced coupling constants indicating a slight deviation of the backbone dihedral angles from idealized values on the N-terminal side of the fluorinated residue. Because, despite their shortness, both tetrapeptides show the anticipated hairpin as the dominant conformation in solution, no conclusions about the potential additional stabilization of the turn by an  $\alpha$ -F-substituent antiperiplanar to the C=O bond can be drawn at this point.

The novel  $\beta$ -peptides of type **4a** turn out to be the simplest hairpin-turn-forming compounds in the world of  $\beta$ -peptides so far; they are expected to be welcome scaffolds for imitating the structure and for mimicking the biological affinities of  $\alpha$ -peptidic hairpin turns.

#### Experimental Part

1. *General Abbreviations*: DBU: 1,8-Diazabicyclo[5.4.0]undec-7-ene, HATU: *O*-(7-azabenzotriazol-1-yl)-*N,N,N',N'*-tetramethyluronium hexafluorophosphate, HPLC: high-performance liquid chromatography, h.v.: high vacuum (0.01–0.1 Torr), MALDI: matrix-assisted laser desorption ionization, TFA: CF<sub>3</sub>COOH, TNBS: 2,4,6-trinitrobenzenesulfonic acid. *Wang* and *Rink* amide AM resin were purchased from *NovaBiochem*. Fmoc- $\beta^3$ -amino acids were purchased from *Fluka*. Anal. reversed-phase (RP) HPLC: on a *Merck/Hitachi* HPLC system (*LaChrom*, pump type *L-7150*, UV detector *L-7400*, interface *D-7000*, HPLC manager *D-7000*). *Macherey-Nagel* C<sub>8</sub>-column (*Nucleosil 100-5 C<sub>8</sub>* (250 × 4 mm), C<sub>18</sub> column (*Nucleosil 100-5 C<sub>18</sub>* (250 × 4 mm), using a gradient of *A* (MeCN) and *B* (0.1% TFA in H<sub>2</sub>O) at a flow rate of 1 ml/min. Prep. HPLC: *Merck/Hitachi* HPLC system (*LaChrom*, pump type *L-7150*, UV detector *L-7400*, interface *D-7000*, HPLC manager *D-7000*). *Macherey-Nagel* C<sub>8</sub>-column (*Nucleosil 100-7 C<sub>8</sub>* (250 × 21 mm), C<sub>18</sub> column (*Nucleosil 100-7 C<sub>18</sub>* (250 × 21 mm) using a gradient of *A* (MeCN) and *B* (0.1% TFA in H<sub>2</sub>O) at a flow rate of 10 ml/min. Retention time (*t<sub>R</sub>*) given in min. TFA for anal. and prep. HPLC was of UV-grade quality (> 99% GC). Lyophilization: *Hetosicc* cooling condenser with h.v. pump to obtain the peptides as their TFA salts. NMR Spectra: chemical shifts  $\delta$  are given in ppm relative to resonances of solvent (<sup>1</sup>H: 3.31 ppm for CD<sub>3</sub>OD; <sup>13</sup>C: 49.15 ppm for CD<sub>3</sub>OD), coupling constants *J* are given in (Hz). For multiplets, the center of the signal is given. The multiplicities of signals was determined by DEPT: DEPT: += primary or tertiary (positive DEPT signal), -= secondary (negative DEPT signal), C<sub>q</sub> = quaternary C-atoms. MS: *IonSpec Ultima 4.7T FT* ion cyclotron resonance (ICR, HR-MALDI, in a 2,5-dihydroxybenzoic acid matrix) mass spectrometer; in *m/z* (% of basis peak).

2. *General Procedures for Peptide Synthesis*. 2.1. *N-Acylation* (‘capping’) of *Peptides*. *General Procedure I (GP I)*. A soln. of Ac<sub>2</sub>O (1 ml) in DMF (2.5 ml) was added to the resin, followed by a soln. of



DMAP (50 mg) in DMF (2.5 ml), and the suspension was mixed by N<sub>2</sub> bubbling for 1 h. The resin was filtered and washed with DMF (4 ml, 3 × 1 min) and CH<sub>2</sub>Cl<sub>2</sub> (4 ml, 5 × 1 min), and dried under h.v. for 12 h.

2.2. Wang and Rink Amide AM Resin Cleavage and Final Deprotection. General Procedure 2 (GP 2). The dried peptide resin was suspended in a soln. of TFA/H<sub>2</sub>O/(i-Pr)<sub>3</sub>SiH 95 : 2.5 : 2.5 (10 ml) for 2 h. The resin was removed by filtration and washed with TFA (2 ×). The filtrates were combined, and the volatiles were removed under reduced pressure. The resulting oily residue was treated with cold Et<sub>2</sub>O to precipitate the crude peptide as the TFA salt.

2.3. Synthesis of Peptides **1–3**. *H*-(*R*)-β<sup>3</sup>hSer-(*S*)-β<sup>3</sup>hLeu-(*S*)-β<sup>3</sup>hGlu-(*R*)-β<sup>3</sup>hVal-(*R*)-β<sup>3</sup>hIle-(*S*)-β<sup>3</sup>hLys-(*S,S*)-β<sup>2,3</sup>hAla(αF)-(*S*)-β<sup>3</sup>hPhe-(*S*)-β<sup>3</sup>hAsn-(*R*)-β<sup>3</sup>hVal-(*S*)-β<sup>3</sup>hAla-(*S*)-β<sup>3</sup>hTyr-(*S*)-β<sup>3</sup>hAla-OH (**1**). In a reactor, Fmoc-β<sup>3</sup>hAla-Wang resin (258 mg, 150 μmol, 0.58 mmol/g) was swollen in DMF (5 ml) for 30 min. The resin was filtered and washed with DMF (5 × 5 ml, 1 min). Fmoc-Deprotection was carried out using piperidine/DMF (20%, 5 ml, 3 × 10 min) under N<sub>2</sub> bubbling. The resin was filtered and washed with DMF (5 ml, 5 × 1 min), CH<sub>2</sub>Cl<sub>2</sub> (5 ml, 5 × 1 min), and DMF (5 ml, 5 × 1 min). For each coupling step, a soln. of the corresponding Fmoc-β-amino acid (450 μmol, 3 equiv.), HATU (165 mg, 435 μmol, 2.9 equiv.), and EtN(i-Pr)<sub>2</sub> (154 μl, 900 μmol, 6 equiv.) in 10 ml of DMF was added to the resin, and the suspension was mixed by N<sub>2</sub> bubbling for 1 h. Each coupling step was monitored with TNBS [37] and, if necessary, the coupling time was prolonged to 2 h. For the coupling of the valuable (2*S*,3*S*)-3-(((9*H*-Fluoren-9-yl)methoxy)carbonyl)amino)-2-fluoropropanoic acid, 2 equiv. were used, and the coupling time was prolonged to 2 h. The resin was washed with DMF (5 ml, 5 × 1 min), CH<sub>2</sub>Cl<sub>2</sub> (5 ml, 5 × 1 min), and DMF (5 ml, 5 × 1 min), prior to Fmoc-deprotection. After the removal of the last Fmoc protecting group, the resin was washed with DMF (5 ml, 5 × 1 min) and CH<sub>2</sub>Cl<sub>2</sub> (5 ml, 5 × 1 min), and dried under h.v. for 12 h. Cleavage of the peptide from the resin and side-chain deprotection was carried out according to GP 2. Removal of the volatiles under reduced pressure and precipitation of the peptide with cold Et<sub>2</sub>O, followed by centrifugation, gave the crude peptide. Purification by prep. RP-HPLC (10% A for 5 min, 10–90% A in 40 min), followed by lyophilization, yielded 27 mg of (**1**) (10%) as a TFA salt. Colorless solid. Anal. RP-HPLC (10–95% A in 45 min): *t*<sub>R</sub> 21.54, purity > 95%. <sup>1</sup>H-NMR (600 MHz, CD<sub>3</sub>OH): 0.93 (*d*, *J* = 6.9, Me, β<sup>3</sup>hVal<sup>10</sup>); 0.95 (*d*, *J* = 6.6, Me, β<sup>3</sup>hLeu<sup>2</sup>); 0.96 (*d*, *J* = 6.8, Me, β<sup>3</sup>hVal<sup>4</sup>); 1.00 (*m*, CH<sub>2</sub>, β<sup>3</sup>hIle<sup>5</sup>); 1.13 (*d*, *J* = 6.6, Me, β<sup>3</sup>hAla<sup>13</sup>); 1.17 (*d*, *J* = 6.7, Me, β<sup>3</sup>hAla<sup>11</sup>); 1.24 (*d*, *J* = 5.7, Me, β<sup>2,3</sup>hAla(αF)); 1.34 (*m*, 1 H, CH<sub>2</sub>, β<sup>3</sup>hLeu<sup>2</sup>); 1.44 (*m*, CH<sub>2</sub>, β<sup>3</sup>hLys<sup>6</sup>); 1.53 (*m*, 1 H, CH<sub>2</sub>, β<sup>3</sup>hLeu<sup>2</sup>); 1.60 (*m*, CH, β<sup>3</sup>hIle<sup>5</sup>); 1.63 (*m*, CH, β<sup>3</sup>hLeu<sup>2</sup>); 1.63 (*m*, CH<sub>2</sub>, β<sup>3</sup>hLys<sup>6</sup>); 1.65 (*m*, CH<sub>2</sub>, β<sup>3</sup>hLys<sup>6</sup>); 1.74 (*m*, CH, β<sup>3</sup>hVal<sup>10</sup>); 1.75 (*m*, 1 H, CH<sub>2</sub>, β<sup>3</sup>hGlu<sup>3</sup>); 1.80 (*m*, CH, β<sup>3</sup>hVal<sup>4</sup>); 1.87 (*m*, 1 H, CH<sub>2</sub>, β<sup>3</sup>hGlu<sup>3</sup>); 2.29 (*m*, 1 H, CH<sub>2</sub>, β<sup>3</sup>hTyr<sup>12</sup>); 2.33 (*m*, 1 H, CH<sub>2</sub>, β<sup>3</sup>hPhe<sup>8</sup>); 2.34 (*m*, CH<sub>2</sub>, β<sup>3</sup>hAla<sup>11</sup>); 2.36 (*m*, 1 H, CH<sub>2</sub>, β<sup>3</sup>hGlu<sup>3</sup>); 2.43 (*m*, 1 H, CH<sub>2</sub>, β<sup>3</sup>hVal<sup>4</sup>); 2.43 (*m*, 1 H, CH<sub>2</sub>, β<sup>3</sup>hVal<sup>10</sup>); 2.44 (*m*, 1 H, CH<sub>2</sub>, β<sup>3</sup>hAsn<sup>9</sup>); 2.48 (*m*, 1 H, CH<sub>2</sub>, β<sup>3</sup>hLeu<sup>2</sup>); 2.48 (*m*, 1 H, CH<sub>2</sub>, β<sup>3</sup>hGlu<sup>3</sup>); 2.51 (*m*, 1 H, CH<sub>2</sub>, β<sup>3</sup>hAsn<sup>9</sup>); 2.52 (*m*, CH<sub>2</sub>, β<sup>3</sup>hAla<sup>13</sup>); 2.53 (*m*, 1 H, CH<sub>2</sub>, β<sup>3</sup>hLys<sup>6</sup>); 2.59 (*m*, 1 H, CH<sub>2</sub>, β<sup>3</sup>hTyr<sup>12</sup>); 2.59 (*m*, 1 H, CH<sub>2</sub>, β<sup>3</sup>hSer<sup>1</sup>); 2.61 (*m*, CH<sub>2</sub>, β<sup>3</sup>hIle<sup>5</sup>); 2.61 (*m*, 1 H, CH<sub>2</sub>, β<sup>3</sup>hTyr<sup>12</sup>); 2.63 (*m*, 1 H, CH<sub>2</sub>, β<sup>3</sup>hAsn<sup>9</sup>); 2.63 (*m*, 1 H, CH<sub>2</sub>, β<sup>3</sup>hPhe<sup>8</sup>); 2.72 (*m*, 1 H, CH<sub>2</sub>, β<sup>3</sup>hVal<sup>4</sup>); 2.73 (*m*, 1 H, CH<sub>2</sub>, β<sup>3</sup>hVal<sup>10</sup>); 2.77 (*m*, 1 H, CH<sub>2</sub>, β<sup>3</sup>hAsn<sup>9</sup>); 2.79 (*m*, 1 H, CH<sub>2</sub>, β<sup>3</sup>hTyr<sup>12</sup>); 2.83 (*m*, 1 H, CH<sub>2</sub>, β<sup>3</sup>hLys<sup>6</sup>); 2.85 (*m*, 1 H, CH<sub>2</sub>, β<sup>3</sup>hLeu<sup>2</sup>); 3.06 (*m*, 1 H, CH<sub>2</sub>, β<sup>3</sup>hSer<sup>1</sup>); 3.71 (*m*, 2 H, β<sup>3</sup>hSer<sup>1</sup>); 3.83 (*m*, 1 H, CH<sub>2</sub>, β<sup>3</sup>hSer<sup>1</sup>); 4.28 (*m*, CH, β<sup>3</sup>hIle<sup>5</sup>); 4.30 (*m*, CH, β<sup>3</sup>hVal<sup>10</sup>); 4.32 (*m*, CH, β<sup>3</sup>hVal<sup>4</sup>); 4.34 (*m*, CH, β<sup>3</sup>hGlu<sup>3</sup>); 4.40 (*m*, CH, β<sup>3</sup>hAla<sup>13</sup>); 4.41 (*m*, CH, β<sup>3</sup>hAla<sup>11</sup>); 4.46 (*m*, β<sup>3</sup>hLeu<sup>2</sup>); 4.80 (*m*, CH, β<sup>3</sup>hTyr<sup>12</sup>); 4.57 (*m*, CH, β<sup>2,3</sup>hAla(αF)); 4.63 (*m*, CH, β<sup>3</sup>hPhe<sup>8</sup>); 4.64 (*m*, CH, β<sup>3</sup>hLeu<sup>2</sup>); 4.80 (*m*, CH, β<sup>3</sup>hAsn<sup>9</sup>); 5.10 (*dd*, *J* = 48.0, 10.0, 1 H, β<sup>2,3</sup>hAla(αF)); 6.68 (*d*, *J* = 8.5, 2 H, β<sup>3</sup>hTyr<sup>12</sup>); 7.02 (*d*, *J* = 8.5, 2 H, β<sup>3</sup>hTyr<sup>12</sup>); 7.15 (*d*, *J* = 7.3, 2 H, β<sup>3</sup>hPhe<sup>8</sup>); 7.22 (*t*, *J* = 7.3, 1 H, β<sup>3</sup>hPhe<sup>8</sup>); 7.27 (*d*, *J* = 7.3, 2 H, β<sup>3</sup>hPhe<sup>8</sup>); 7.56 (*d*, *J* = 8.9, NH, β<sup>3</sup>hAla<sup>11</sup>); 7.73 (*d*, *J* = 9.5, NH, β<sup>3</sup>hTyr<sup>12</sup>); 7.85 (*d*, *J* = 8.5, NH, β<sup>3</sup>hAla<sup>13</sup>); 7.92 (*d*, *J* = 9.3, NH, β<sup>3</sup>hIle<sup>5</sup>); 7.95 (*d*, *J* = 9.4, NH, β<sup>3</sup>hVal<sup>10</sup>); 8.13 (*d*, *J* = 9.3, NH, β<sup>3</sup>hLys<sup>6</sup>); 8.36 (*d*, *J* = 9.5, NH, β<sup>3</sup>hLeu<sup>2</sup>); 8.39 (*d*, *J* = 9.1, NH, β<sup>3</sup>hVal<sup>4</sup>); 8.41 (*d*, *J* = 9.1, NH, β<sup>3</sup>hAsn<sup>9</sup>); 8.55 (*d*, *J* = 9.1, NH, β<sup>3</sup>hGlu<sup>3</sup>); 8.69 (*d*, *J* = 9.7, NH, β<sup>2,3</sup>hAla(αF)); 8.78 (*d*, *J* = 9.1, NH, β<sup>3</sup>hPhe<sup>8</sup>). <sup>13</sup>C-NMR (125 MHz, CD<sub>3</sub>OH): 12.4; 16.2; 18.3; 19.3; 19.4; 19.5; 19.8; 21.2; 21.4; 22.9; 23.5; 24.4; 26.3; 27.5; 28.8; 32.7; 34.2; 34.3; 36.4; 36.7; 38.2; 38.7; 38.9; 40.8; 40.9; 41.0; 41.2; 41.5; 41.6; 41.6; 41.7; 42.4; 42.6; 43.0; 43.2; 43.4; 43.6; 45.2; 45.9; 46.0; 46.1; 46.7; 47.1; 48.0; 49.0; 49.5; 52.7; 52.8; 52.8; 52.9; 63.2; 93.6; 94.7; 116.2; 127.8; 129.6; 130.3; 130.6; 131.7; 138.7; 157.3; 168.3; 168.4; 171.0; 171.3; 171.7; 171.8; 171.9; 172.1; 172.3; 172.4; 172.4; 174.0; 177.4. For NOEs, cf. Table 6. MALDI-MS: 1664.9 (25), 1663.9 (30), 1662.9 (33, [M + K]<sup>+</sup>).

Table 6. NOEs Observed in the 300-ms ROESY Spectrum of **1** in CD<sub>3</sub>OH<sup>a</sup>)

Residue	H-Atom	Residue	H-Atom	$d_{\text{NOE}}$ [Å]	Residue	H-Atom	Residue	H-Atom	$d_{\text{NOE}}$ [Å]
1	$\alpha_{\text{Re}}$	1	$\alpha_{\text{Si}}$	1.9	1	$\alpha^*$	2	HN	2.9
1	$\beta$	1	$\alpha^*$	3.0	2	HN	3	HN	4.3
2	$\beta$	2	$\gamma^*$	3.2	4	HN	5	HN	4.3
2	$\beta$	2	HN	2.9	5	HN	6	HN	4.2
2	$\delta$	2	HN	3.4	6	$\alpha^*$	7	HN	2.9
2	$\gamma^1$	2	$\gamma^2$	2.0	6	HN	6	HN	4.4
3	$\alpha$	3	HN	3.2	7	$\alpha$	8	HN	2.5
3	$\gamma^*$	3	$\beta$	3.2	8	HN	9	HN	4.2
3	$\beta$	3	HN	3.1	9	HN	10	HN	4.3
4	$\beta$	4	HN	2.9	10	HN	11	HN	4.4
4	$\beta$	4	$\gamma$	2.5	11	$\alpha^*$	12	HN	3.0
4	$\gamma$	4	HN	3.2	12	HN	13	$\beta$	5.0
5	$\gamma$	5	HN	2.8	13	HN	12	$\alpha^*$	2.9
5	$\beta$	5	HN	2.9	1	$\alpha^*$	4	$\beta$	2.8
5	$\alpha^*$	5	HN	3.2	1	$\gamma^*$	4	$\beta$	3.9
6	$\alpha^*$	6	HN	3.2	2	$\gamma^*$	5	$\beta$	3.3
6	$\beta$	6	HN	3.0	3	HN	5	HN	4.9
7	$\alpha$	7	HN	2.7	3	HN	6	$\beta$	3.5
7	$\gamma^*$	7	$\alpha$	3.0	3	$\gamma^*$	6	$\beta$	3.9
7	$\gamma^*$	7	$\beta$	3.0	4	HN	6	HN	5.0
7	$\gamma^*$	7	HN	3.4	4	$\alpha^*$	7	$\alpha$	3.0
8	$\alpha^*$	8	HN	3.2	4	$\gamma$	7	$\alpha$	3.8
8	$\alpha^*$	8	$\beta$	2.8	4	$\gamma$	7	$\beta$	3.7
8	$\gamma^*$	8	$\beta$	3.0	4	HN	7	$\alpha$	3.8
8	$\beta$	8	HN	3.0	4	$\gamma$	7	$\gamma^*$	4.5
8	$\gamma^1$	8	$\gamma^2$	2.0	5	HN	8	$\beta$	3.2
9	$\alpha^*$	9	HN	3.2	6	HN	8	$\beta$	3.4
9	$\gamma^*$	9	$\beta$	3.2	6	$\alpha^*$	9	$\beta$	3.1
9	$\beta$	9	HN	3.0	7	$\alpha$	10	$\beta$	2.8
10	$\gamma$	10	$\beta$	2.5	7	$\gamma^*$	10	$\beta$	3.5
10	$\beta$	10	HN	2.9	7	$\gamma^*$	10	$\gamma$	4.5
10	$\gamma$	10	HN	3.2	7	HN	10	$\beta$	3.0
11	$\alpha^*$	11	HN	3.2	8	HN	10	$\beta$	3.6
11	$\gamma^*$	11	$\beta$	3.0	8	HN	11	$\beta$	3.0
11	$\beta$	11	HN	3.0	9	$\beta$	6	HN	3.8
11	$\gamma^*$	11	HN	3.5	9	$\beta$	7	HN	3.9
12	$\beta$	12	HN	3.0	9	HN	11	$\beta$	3.5
12	$\alpha^*$	12	HN	3.1	10	$\beta$	6	HN	4.6
12	$\gamma^*$	12	HN	3.5	10	HN	7	HN	4.7
13	$\alpha^*$	13	HN	3.1	10	HN	8	HN	4.6
13	$\gamma^*$	13	$\beta$	3.0	10	HN	13	$\beta$	3.1
13	$\beta$	13	HN	3.0	12	$\beta$	9	HN	2.8
13	$\gamma^*$	13	HN	3.6	12	$\beta$	10	HN	3.8
1	$\beta$	2	HN	4.3	13	$\gamma^*$	10	$\gamma$	5.0

<sup>a</sup>) \* = Pseudoatom used for calculations.

1650.0 (13), 1649.0 (54), 1648.0 (95), 1647.0 (100,  $[M + Na]^+$ ), 1628.0 (15), 1627.0 (38), 1626.0 (51), 1625.0 (56,  $[M + H]^+$ ). HR-MS: 1646.9555 ( $[M + Na]^+$ ,  $C_{80}H_{130}FN_{15}NaO_{19}$ ; calc. 1646.9549).

*Ac-(2R,3S)- $\beta^2$ -hVal( $\alpha$ Me)-(2S)- $\beta^2$ -hPhe( $\alpha$ F)-(R)- $\beta^3$ -hLys-(2R,3S)- $\beta^2$ - $\beta^3$ -Ala( $\alpha$ Me)-NH<sub>2</sub> (2) and Ac-(2R,3S)- $\beta^2$ -hVal( $\alpha$ Me)-(2R)- $\beta^2$ -hPhe-(R)- $\beta^3$ -hLys-(2R,3S)- $\beta^2$ - $\beta^3$ -Ala( $\alpha$ Me)-NH<sub>2</sub> (3). Rink amide AM resin (169 mg, 0.71 mmol/g, 0.12 mmol) was swollen in CH<sub>2</sub>Cl<sub>2</sub> for 30 min and Fmoc-deprotected with 20% piperidine in DMF (3 ml, 3  $\times$  10 min) under N<sub>2</sub> bubbling. The resin was washed with DMF (4 ml, 3  $\times$  1 min). The first  $\beta$ -amino acid was anchored onto the resin with a soln. of Fmoc-(2R,3S)- $\beta^2$ -hAla( $\alpha$ Me)-OH (122 mg, 0.36 mmol), HATU (123 mg, 0.32 mmol), and EtN(i-Pr)<sub>2</sub> (0.12 ml, 0.72 mmol) in DMF (4 ml). After mixing the suspension for 1 h by N<sub>2</sub> bubbling, the resin was filtered and washed with DMF (4 ml, 5  $\times$  1 min). Completion of the coupling was confirmed by TNBS [37]. In case of a positive TNBS test (indicating incomplete coupling), the resin was treated with the same amino acid (2 equiv.) and coupling reagents. The second amino acid was coupled using Fmoc-(R)- $\beta^3$ -hLys(Boc)-OH (174 mg, 0.36 mmol), HATU (123 mg, 0.32 mmol), EtN(i-Pr)<sub>2</sub> (0.12 ml, 0.72 mmol) in DMF (4 ml), and N<sub>2</sub> mixing for 1 h. After TNBS test, the resin was washed with DMF (4 ml, 3  $\times$  1 min) and CH<sub>2</sub>Cl<sub>2</sub> (4 ml, 3  $\times$  1 min), and dried under h.v. for 1 h to give 220 mg of peptide resin. A portion of the peptide resin (110 mg) was swollen in DMF for 1 h and Fmoc-deprotected with 20% piperidine in DMF (3 ml, 3  $\times$  10 min) by N<sub>2</sub> bubbling. The resin was filtered and washed with DMF (4 ml, 5  $\times$  1 min). Fmoc-(2S)- $\beta^2$ -hPhe( $\alpha$ F)-OH (76 mg, 0.18 mmol) was then coupled using HATU (62 mg, 0.16 mmol) and EtN(i-Pr)<sub>2</sub> (0.06 ml, 0.36 mmol) with N<sub>2</sub> bubbling for 1 h. After TNBS test and Fmoc-deprotection with 20% piperidine in DMF (3 ml, 3  $\times$  10 min), the resin was filtered and washed with DMF (4 ml, 5  $\times$  1 min). Fmoc-(2R,3S)- $\beta^2$ -Val( $\alpha$ Me)-OH (66 mg, 0.18 mmol) was then coupled using HATU (62 mg, 0.16 mmol) and EtN(i-Pr)<sub>2</sub> (0.06 ml, 0.36 mmol) with N<sub>2</sub> bubbling for 1 h. After TNBS test, Fmoc-deprotection was carried out with 20% piperidine in DMF (3 ml, 3  $\times$  10 min). TNBS Test indicated incomplete deprotection, and the resin was treated with DBU/piperidine/DMF (1:1:48) (3 ml, 3  $\times$  1 min). The resin was then filtered and washed with DMF (4 ml, 5  $\times$  1 min). Acylation of the peptide was carried out according to *GP 1*, and the peptide was cleaved from the resin according to *GP 2* to give 43 mg of crude **2**. Purification by prep. RP-HPLC (10% *A* for 5 min, 10–45% *A* in 35 min), followed by lyophilization, gave **2** (12 mg) as a TFA salt. Colorless solid. Anal. RP-HPLC (5–50% *A* in 45 min): *t*<sub>R</sub> 21.56, purity > 98%. <sup>1</sup>H-NMR (600 MHz, CD<sub>3</sub>OH): 0.80 (*m*, CH<sub>2</sub>, (R)- $\beta^3$ -hLys); 0.88 (*d*, *J* = 6.7, Me,  $\beta^2$ -hVal( $\alpha$ Me)); 0.92 (*d*, *J* = 6.8, Me,  $\beta^2$ -hVal( $\alpha$ Me)); 1.11 (*m*, 3 Me,  $\beta^2$ -hAla( $\alpha$ Me),  $\beta^2$ -hVal( $\alpha$ Me),  $\beta^2$ -hAla( $\alpha$ Me)); 1.21 (*m*, 1 H, CH<sub>2</sub>, (R)- $\beta^3$ -hLys); 1.30 (*m*, 1 H, CH<sub>2</sub>, (R)- $\beta^3$ -hLys); 1.45 (*m*, CH<sub>2</sub>, (R)- $\beta^3$ -hLys); 1.80 (*m*, CH,  $\beta^2$ -hVal( $\alpha$ Me)); 1.99 (*s*, MeCO); 2.22 (*dd*, *J* = 14.1, 8.1, 1 H, (R)- $\beta^3$ -hLys); 2.32 (*dd*, *J* = 14.1, 5.1, 1 H, (R)- $\beta^3$ -hLys); 2.42 (*m*, CH,  $\beta^2$ -hAla( $\alpha$ Me)); 2.46 (*m*, CH<sub>2</sub>, (R)- $\beta^3$ -hLys); 2.71 (*m*, CH,  $\beta^2$ -hVal( $\alpha$ Me)); 2.74 (*m*, CH<sub>2</sub>,  $\beta^2$ -Phe( $\alpha$ F)); 3.10 (*m*, 1 H, CH,  $\beta^2$ -Phe); 3.55 (*m*, 1 H, CH<sub>2</sub>,  $\beta^2$ -Phe( $\alpha$ F)); 3.92 (*m*, 1 H, CH<sub>2</sub>,  $\beta^2$ -Phe( $\alpha$ F)); 4.03 (*m*, CH,  $\beta^2$ -hAla( $\alpha$ Me)); 4.04 (*m*, CH, (R)- $\beta^3$ -hLys); 4.13 (*m*, CH,  $\beta^2$ -hVal( $\alpha$ Me)); 7.25 (*m*, 5 arom. H,  $\beta^2$ -Phe( $\alpha$ F)); 7.65 (*d*, *J* = 10.3, NH,  $\beta^2$ -hVal( $\alpha$ Me)); 7.82 (*m*, NH, (R)- $\beta^3$ -hLys); 7.89 (*d*, *J* = 8.8, NH,  $\beta^2$ -hAla( $\alpha$ Me)); 8.32 (*m*, NH,  $\beta^2$ -Phe( $\alpha$ F)). <sup>13</sup>C-NMR (125 MHz, CD<sub>3</sub>OH): 15.3 ( $\beta^2$ -hVal( $\alpha$ Me)); 15.4 (Me,  $\beta^2$ -hAla( $\alpha$ Me)); 16.9 ( $\beta^2$ -hVal( $\alpha$ Me)); 18.5 (Me,  $\beta^2$ -hAla( $\alpha$ Me)); 21.0 (Me,  $\beta^2$ -hVal( $\alpha$ Me)); 22.6 (MeCO); 23.3 (CH<sub>2</sub>, (R)- $\beta^3$ -hLys); 28.3 (CH<sub>2</sub>, (R)- $\beta^3$ -hLys); 31.3 (CH,  $\beta^2$ -hVal( $\alpha$ Me)); 34.5 (CH<sub>2</sub>, (R)- $\beta^3$ -hLys); 40.8 (CH<sub>2</sub>, (R)- $\beta^3$ -hLys); 42.1, 44.4 (CH<sub>2</sub>,  $\beta^2$ -Phe( $\alpha$ F)); 44.3 (CH,  $\beta^2$ -hVal( $\alpha$ Me)); 46.6 (CH,  $\beta^2$ -hAla( $\alpha$ Me)); 47.8 ( $\beta^2$ -hAla( $\alpha$ Me)); 48.3 (CH<sub>2</sub>, (R)- $\beta^3$ -hLys); 48.6 (CH<sub>2</sub>,  $\beta^2$ -Phe( $\alpha$ F)); 48.8 ( $\beta^2$ -hAla( $\alpha$ Me)); 57.4 (CH,  $\beta^2$ -hVal( $\alpha$ Me)); 99.3, 100.6 (CH<sub>2</sub>,  $\beta^2$ -Phe( $\alpha$ F)); 128.1 (arom. C); 129.3 (arom. C); 131.8 (arom. C); 136.2 (arom. C); 172.6 (C=O); 173.8 (C=O); 178.3 (C=O); 178.8 (C=O); 179.9 (C=O). For NOEs, cf. Table 7. ESI-MS: 629.2 ( $[M + Na]^+$ ), 607.2 ( $[M + H]^+$ ). MALDI-MS: 629.4 (6,  $[M + Na]^+$ ), 607.4 (20,  $[M + H]^+$ ), 570.4 (14). HR-MS: 607.3968 ( $C_{51}H_{52}FN_6O_5$ ; calc. 607.3983).*

A further portion of Fmoc-dipeptide resin (110 mg) was swollen in DMF for 1 h and Fmoc-deprotected with 20% piperidine in DMF (3 ml, 3  $\times$  10 min) by N<sub>2</sub> bubbling. The resin was filtered and washed with DMF (4 ml, 5  $\times$  1 min). Fmoc-(2R)- $\beta^2$ -Phe-OH (72 mg, 0.18 mmol) was then coupled using HATU (62 mg, 0.16 mmol) and EtN(i-Pr)<sub>2</sub> (0.06 ml, 0.36 mmol) with N<sub>2</sub> bubbling for 1 h. After TNBS test and Fmoc-deprotection with 20% piperidine in DMF (3 ml, 3  $\times$  10 min), the resin was filtered and washed with DMF (4 ml, 5  $\times$  1 min). Fmoc-(2R,3S)- $\beta^2$ -Val( $\alpha$ Me)-OH (66 mg, 0.18 mmol) was then coupled using HATU (62 mg, 0.16 mmol) and EtN(i-Pr)<sub>2</sub> (0.06 ml, 0.36 mmol) with N<sub>2</sub> bubbling for 1 h.

Table 7. NOEs Observed in the 300-ms ROESY Spectrum of **2** in CD<sub>3</sub>OH<sup>a</sup>)

Residue	H-Atom	Residue	H-Atom	$d_{\text{NOE}}$ [Å]	Residue	H-Atom	Residue	H-Atom	$d_{\text{NOE}}$ [Å]
2	$\beta$	2	$\alpha$	2.9	4	$\beta$	4	HN	3.0
2	$\alpha$	2	$\gamma$	3.1	5	$\alpha$	5	$\beta$	2.8
2	$\alpha$	2	HN	2.7	5	$\alpha$	5	HN	3.0
2	$\beta$	2	$\gamma$	2.6	5	$\beta$	5	HN	2.9
2	$\beta$	2	HN	3.0	2	$\alpha$	3	HN	2.4
2	$\alpha\text{Me}$	2	$\alpha$	2.9	2	$\beta$	3	HN	3.2
2	$\gamma$	2	HN	3.3	3	HN	2	$\gamma$	3.8
3	$\beta_{\text{Si}}$	3	$\beta_{\text{Re}}$	2.0	3	HN	2	$\alpha\text{Me}$	3.9
3	$\beta_{\text{Si}}$	3	HN	3.0	3	HN	4	HN	3.9
3	$\beta_{\text{Si}}$	3	HN	2.9	4	$\alpha_{\text{Re}}$	5	HN	2.7
4	$\alpha_{\text{Si}}$	4	$\beta$	2.8	4	$\alpha_{\text{Si}}$	5	HN	2.9
4	$\beta$	4	$\alpha_{\text{Re}}$	2.6	2	$\alpha$	5	$\beta$	3.1
4	$\alpha_{\text{Si}}$	4	HN	2.9	3	HN	5	$\beta$	3.8
4	$\alpha_{\text{Re}}$	4	HN	3.1	2	HN	5	$\beta$	4.0

<sup>a</sup>) \* = Pseudoatom used for calculations.

After TNBS test, Fmoc-deprotection was carried out with 20% piperidine in DMF (3 ml, 3 × 10 min). Acylation of the peptide was carried out according to *GP 1*, and the peptide was cleaved from the resin according to *GP 2* to give 42 mg of crude **3**. Purification by prep HPLC (10% *A* for 5 min, 10–45% *A* in 35 min) gave **3** (21.2 mg) as a TFA salt. Colorless solid. Anal. RP-HPLC (5–50% *A* in 45 min):  $t_{\text{R}}$  21.05, purity > 98%. <sup>1</sup>H-NMR (600 MHz, CD<sub>3</sub>OH): 0.85 (*m*, CH<sub>2</sub>, (*R*)- $\beta^3$ hLys); 0.89 (*d*,  $J$  = 6.8, Me,  $\beta^{2,3}$ hVal( $\alpha$ Me)); 0.92 (*d*,  $J$  = 6.8, Me,  $\beta^{2,3}$ hVal( $\alpha$ Me)); 1.08 (*d*,  $J$  = 6.8, Me,  $\beta^{2,3}$ hAla( $\alpha$ Me)); 1.10 (*d*,  $J$  = 6.8, Me,  $\beta^{2,3}$ hVal( $\alpha$ Me)); 1.11 (*d*,  $J$  = 6.7, Me,  $\beta^{2,3}$ hAla( $\alpha$ Me)); 1.18 (*m*, 1 H, CH<sub>2</sub>, (*R*)- $\beta^3$ hLys); 1.35 (*m*, 1 H, CH<sub>2</sub>, (*R*)- $\beta^3$ hLys); 1.42 (*m*, 1 H, CH<sub>2</sub>, (*R*)- $\beta^3$ hLys); 1.46 (*m*, 1 H, CH<sub>2</sub>, (*R*)- $\beta^3$ hLys); 1.79 (*m*, CH,  $\beta^{2,3}$ hVal( $\alpha$ Me)); 1.99 (*s*, MeCO); 2.21 (*dd*,  $J$  = 14.0, 7.7, 1 H, (*R*)- $\beta^3$ hLys); 2.28 (*dd*,  $J$  = 14.0, 6.0, 1 H, (*R*)- $\beta^3$ hLys); 2.42 (*m*, CH,  $\beta^{2,3}$ hAla( $\alpha$ Me)); 2.61 (*m*, CH,  $\beta^{2,3}$ hVal( $\alpha$ Me)); 2.74 (*m*, CH<sub>2</sub>,  $\beta^2$ Phe); 2.78 (*m*, CH,  $\beta^2$ Phe); 2.79 (*m*, CH<sub>2</sub>, (*R*)- $\beta^3$ hLys); 3.31 (*m*, 1 H, CH<sub>2</sub>,  $\beta^2$ Phe); 3.43 (*m*, 1 H, CH<sub>2</sub>,  $\beta^2$ Phe); 4.05 (*m*, CH,  $\beta^{2,3}$ hAla( $\alpha$ Me)); 4.06 (*m*, 1 H, CH<sub>2</sub>, (*R*)- $\beta^3$ hLys); 4.11 (*m*, CH,  $\beta^{2,3}$ hVal( $\alpha$ Me)); 7.18 (*m*, 3 arom. H,  $\beta^2$ Phe); 7.25 (*t*,  $J$  = 7.4, 2 arom. H,  $\beta^2$ Phe); 7.66 (*d*,  $J$  = 10.1, NH,  $\beta^{2,3}$ hVal( $\alpha$ Me)); 7.80 (*d*,  $J$  = 8.9, NH, (*R*)- $\beta^3$ hLys); 7.88 (*d*,  $J$  = 8.8, NH,  $\beta^{2,3}$ hAla( $\alpha$ Me)); 8.32 (*t*,  $J$  = 6.4, NH,  $\beta^2$ Phe). <sup>13</sup>C-NMR (125 MHz, CD<sub>3</sub>OH): 15.3 (+, Me,  $\beta^{2,3}$ hAla( $\alpha$ Me)); 16.9 (+, 2 Me,  $\beta^{2,3}$ hVal( $\alpha$ Me)); 18.6 (+, Me,  $\beta^{2,3}$ hAla( $\alpha$ Me)); 21.0 (+, Me,  $\beta^{2,3}$ hVal( $\alpha$ Me)); 22.6 (+, MeCO); 23.3 (–, CH<sub>2</sub>, (*R*)- $\beta^3$ hLys); 28.2 (–, CH<sub>2</sub>, (*R*)- $\beta^3$ hLys); 31.4 (+, CH,  $\beta^{2,3}$ hVal( $\alpha$ Me)); 34.7 (–, CH<sub>2</sub>, (*R*)- $\beta^3$ hLys); 37.3 (–, CH<sub>2</sub>, (*R*)- $\beta^3$ hLys); 40.8 (–, CH<sub>2</sub>,  $\beta^2$ Phe); 42.8 (–, CH<sub>2</sub>, (*R*)- $\beta^3$ hLys); 43.2 (–, CH<sub>2</sub>,  $\beta^2$ Phe); 44.3 (+, CH,  $\beta^{2,3}$ hVal( $\alpha$ Me)); 46.7 (+, CH,  $\beta^{2,3}$ hAla( $\alpha$ Me)); 47.8 (+, CH, (*R*)- $\beta^3$ hLys); 48.8 (+, CH,  $\beta^{2,3}$ hAla( $\alpha$ Me)); 50.3 (+, CH,  $\beta^2$ Phe); 57.5 (+, CH,  $\beta^{2,3}$ hVal( $\alpha$ Me)); 127.4 (+, arom. C); 129.5 (+, arom. C); 130.2 (+, arom. C); 140.7 (C<sub>q</sub>, arom. C); 172.5 (C<sub>q</sub>, C=O); 173.8 (C<sub>q</sub>, C=O); 175.2 (C<sub>q</sub>, C=O); 177.9 (C<sub>q</sub>, C=O); 179.9 (C<sub>q</sub>, C=O). For NOEs, cf. Table 8. ESI-MS: 611.1 ([*M* + Na]<sup>+</sup>), 589.3 ([*M* + H]<sup>+</sup>). MALDI-MS: 627.4 (18, [*M* + K]<sup>+</sup>), 612.4 (36), 611.4 (100, [*M* + Na]<sup>+</sup>), 590.4 (26), 589.4 (71, [*M* + H]<sup>+</sup>). HR-MS: 589.4063, (C<sub>31</sub>H<sub>53</sub>N<sub>6</sub>O<sub>3</sub><sup>+</sup>; calc. 589.4077).

3. *NMR Measurements.* The trifluoroacetate salt (H<sub>3</sub>N<sup>+</sup>/COOH form) of  $\beta$ -peptides **1**, and protected forms of peptides **2** and **3**, as well as of the unprotected peptide **4a** (cf. Table 9) were dissolved in CD<sub>3</sub>OH (0.7 ml). All NMR spectra were acquired with presaturation of the solvent OH signal at 600 MHz (<sup>1</sup>H)/150 MHz (<sup>13</sup>C).

DQF-COSY with coherence transfer selection by  $z$ -gradients. TOCSY with 80 ms DIPSI-2 spin lock (8.9 kHz). HSQC with coherence transfer selection by  $z$ -gradients. HMBC with coherence transfer selection by  $z$ -gradients. ROESY: Clean ROESY with 300- and 150-ms CW-spin lock (2.8 kHz). Spectral

Table 8. *NOEs Observed in the 300-ms ROESY Spectrum of 3 in CD<sub>3</sub>OH<sup>a</sup>*

Residue	H-Atom	Residue	H-Atom	$d_{\text{NOE}}$ [Å]	Residue	H-Atom	Residue	H-Atom	$d_{\text{NOE}}$ [Å]
1	$\alpha$	1	$\beta$	2.8	4	$\alpha$	4	HN	3.0
1	$\alpha$	1	$\gamma$	3.0	4	$\beta$	4	HN	2.8
1	$\alpha$	1	HN	2.6	1	$\alpha$	2	HN	2.2
1	$\beta$	1	$\gamma$	2.4	1	$\beta$	2	HN	3.2
1	$\beta$	1	HN	3.0	1	$\alpha\text{Me}$	2	HN	3.9
1	$\alpha\text{Me}$	1	$\beta$	3.0	1	$\gamma$	2	HN	3.7
1	$\gamma$	1	HN	2.9	2	$\beta_{\text{Si}}$	3	HN	3.8
2	$\alpha$	2	HN	3.4	2	$\beta_{\text{Re}}$	3	HN	3.7
2	$\beta_{\text{Si}}$	2	HN	2.6	2	HN	3	HN	3.8
2	$\beta_{\text{Re}}$	2	HN	2.8	3	$\alpha_{\text{Si}}$	4	HN	2.7
3	$\alpha_{\text{Si}}$	3	HN	3.2	3	$\alpha_{\text{Re}}$	4	HN	2.6
3	$\alpha_{\text{Re}}$	3	HN	3.1	3	HN	2	$\alpha$	2.5
3	$\gamma^*$	3	$\beta$	3.3	4	$\beta$	1	$\alpha$	3.2
3	$\beta$	3	HN	3.0	4	$\beta$	2	HN	3.8
4	$\alpha$	4	$\beta$	2.8					

<sup>a</sup>) \* = Pseudoatom used for calculations.

Table 9. *NOEs Observed in the 300-ms ROESY Spectrum of 4a in CD<sub>3</sub>OH<sup>a</sup>*

Residue	H-Atom	Residue	H-Atom	$d_{\text{NOE}}$ [Å]	Residue	H-Atom	Residue	H-Atom	$d_{\text{NOE}}$ [Å]
1	$\alpha_{\text{Si}}$	1	$\gamma$	3.4	4	$\beta$	4	HN	2.9
1	$\alpha_{\text{Re}}$	1	$\gamma$	3.5	4	$\beta$	4	$\gamma^*$	3.1
1	$\beta$	1	$\gamma$	2.9	1	$\alpha_{\text{Si}}$	2	HN	3.1
2	$\beta_{\text{Re}}$	2	$\alpha$	2.5	1	$\alpha_{\text{Re}}$	2	HN	3.2
2	$\alpha$	2	HN	3.5	1	$\beta$	2	HN	5.0
2	$\beta_{\text{Si}}$	2	$\beta_{\text{Re}}$	1.9	2	$\gamma$	3	HN	3.5
2	$\beta_{\text{Re}}$	2	HN	3.3	3	$\alpha_{\text{Re}}$	4	HN	2.5
2	$\beta_{\text{Si}}$	2	HN	3.1	3	$\alpha_{\text{Si}}$	4	HN	2.6
2	$\gamma$	2	HN	4.1	3	$\beta$	4	HN	3.0
3	$\beta_{\text{Si}}$	3	$\beta$	2.4	3	HN	2	$\beta_{\text{Si}}$	4.0
3	$\beta_{\text{Re}}$	3	$\beta$	2.5	3	HN	2	$\beta_{\text{Re}}$	4.7
3	$\beta_{\text{Si}}$	3	HN	3.3	1	$\alpha_{\text{Re}}$	4	$\beta$	3.9
3	$\beta$	3	HN	3.0	1	$\alpha_{\text{Si}}$	4	$\beta$	4.2
4	$\beta$	4	$\alpha^*$	3.0					

<sup>a</sup>) \* = Pseudoatom used for calculations.

width 6000 Hz,  $2k \times 512$  data points acquired (64 scans/FID) with TPPI. Processed with  $\cos^2$  window function to give  $1k \times 1k$  real data points. Polynomial baseline correction in both dimensions.

Assignments and volume integration of ROESY cross-peaks were performed with the aid of SPARKY [38]. Distance constraints and error limits were generated from cross-peak volumes by calibration with known distances (two-spin approximation,  $\pm 20\%$  error limits) through a python extension within SPARKY. The volumes of cross-peaks involving Me groups or other groups of isochronous protons were corrected by division through the number of H-atoms.

4. *Simulated Annealing (SA) Structure Calculations.* Program XPLOR-NIH v2.9.7 [39]. The standard parameter and topology files of XPLOR-NIH (parallhdg.pro; topallhdg.pro) were modified to accommodate  $\beta^3$ -amino acid residues. Minimized extended zig-zag conformations were used as the

starting structures. The SA calculation protocol (adopted from the torsional-angle dynamics protocol of Stein *et al.* [40]) included 4000 steps (0.015 ps each) of high-temp. torsional angle dynamics at 2000 K, followed by 4000 (0.015 ps) steps of slow cooling to 1000 K with torsional-angle dynamics, 4000 steps (0.003 ps) of slow cooling with cartesian dynamics to 300 K, and a final conjugate gradient minimization. The only nonbonded interactions used were *Van der Waals* repel functions. For each compound, 30 structures were calculated. A summary of the calculation statistics is given in *Tables 6–9*.

## REFERENCES

- [1] D. Seebach, A. K. Beck, D. Bierbaum, *Chem. Biodiv.* **2004**, *1*, 1111.
- [2] D. Seebach, D. F. Hook, A. Glättli, *Biopolymers (Peptide Sci.)* **2006**, *84*, 23.
- [3] D. Seebach, R. I. Mathad, T. Kimmerlin, Y. R. Mahajan, P. Bindschädler, M. Rueping, B. Jaun, *Helv. Chim. Acta* **2005**, *88*, 1969.
- [4] a) K. Gademann, A. Häne, M. Rueping, B. Jaun, D. Seebach, *Angew. Chem., Int. Ed.* **2003**, *42*, 1534, b) F. Gessier, C. Noti, M. Rueping, D. Seebach, *Helv. Chim. Acta* **2003**, *86*, 1862, c) D. F. Hook, F. Gessier, C. Noti, P. Kast, D. Seebach, *ChemBioChem* **2004**, *5*, 691, d) R. I. Mathad, F. Gessier, D. Seebach, B. Jaun, *Helv. Chim. Acta* **2005**, *88*, 266.
- [5] M. T. Reetz, M. W. Drewes, K. Harms, W. Reif, *Tetrahedron Lett.* **1988**, *29*, 3295.
- [6] L. Somekh, A. Shanzer, *J. Am. Chem. Soc.* **1982**, *104*, 5836.
- [7] J. W. Banks, A. S. Batsanov, J. A. K. Howard, D. O' Hagan, H. S. Rzepa, S. Martin-Santamaria, *J. Chem. Soc., Perkin Trans. 2* **1999**, 2409.
- [8] D. O. Hughes, R. W. H. Small, *Acta Crystallogr.* **1962**, *15*, 933.
- [9] C. R. S. Briggs, D. O' Hagan, J. A. K. Howard, D. S. Yufit, *J. Fluorine Chem.* **2003**, *119*, 9.
- [10] B. J. van der Veken, S. Truyen, W. A. Herrebout, G. Watkins, *J. Mol. Struct.* **1993**, *293*, 55.
- [11] P. R. Olivato, R. Rittner, 'Reviews on Heteroatom Chemistry', Ed. S. Oae, Vol. 13, MYU, Tokyo, 1996.
- [12] P. R. Olivato, S. A. Guerrero, M. H. Yreijo, R. Rittner, C. F. Tormena, *J. Mol. Struct.* **2002**, *607*, 87.
- [13] E. L. Eliel, S. H. Wilen, 'Stereochemistry of Organic Compounds' John Wiley & Sons New York, 1994, p. 731–734.
- [14] N. E. J. Gooseman, D. O' Hagan, M. J. G. Peach, A. M. Z. Slawan, D. J. Tozer, R. J. Young, *Angew. Chem., Int. Ed.* **2007**, *46*, 5904, and refs. cit. therein.
- [15] H. Brunner, 'Rechts oder links – in der Natur und andersweg', Wiley-VCH, Weinheim, 1999.
- [16] P. I. Arvidsson, M. Rueping, D. Seebach, *Chem. Commun.* **2001**, 649.
- [17] R. P. Cheng, W. F. DeGrado, *J. Am. Chem. Soc.* **2001**, *123*, 5162.
- [18] D. S. Daniels, E. J. Petersson, J. X. Qiu, A. Schepartz, *J. Am. Chem. Soc.* **2007**, *129*, 1532.
- [19] a) D. Seebach, S. Abele, K. Gademann, B. Jaun, *Angew. Chem., Int. Ed.* **1999**, *38*, 1595, b) D. Seebach, J. V. Schreiber, S. Abele, X. Daura, W. F. van Gunsteren, *Helv. Chim. Acta* **2000**, *83*, 34, c) X. Daura, K. Gademann, H. Schäfer, B. Jaun, D. Seebach, W. F. van Gunsteren, *J. Am. Chem. Soc.* **2001**, *123*, 2393.
- [20] G. Lelais, D. Seebach, B. Jaun, R. I. Mathad, O. Flögel, F. Rossi, M. Campo, A. Wortmann, *Helv. Chim. Acta* **2006**, *89*, 361.
- [21] G. Quinkert, E. Egert, C. Griesinger, 'Aspekte der Organischen Chemie. Struktur', Wiley-VCH, Weinheim, 1996; G. Quinkert, E. Egert, C. Griesinger, 'Aspects of Organic Chemistry. Structure', Wiley-VCH, Weinheim, 1996.
- [22] N. Sewald, H.-D. Jakubke, 'Peptides: Chemistry and Biology', Wiley-VCH, Weinheim, 2002.
- [23] A. D. Abell, M. K. F. Edmonds, F. H. M. Graichen, unpublished results, University of Canterbury, Christchurch, New Zealand.
- [24] O. Flögel, J. D. C. Codée, D. Seebach, P. H. Seeberger, *Angew. Chem., Int. Ed.* **2006**, *45*, 7000.
- [25] a) D. Seebach, P. E. Ciceri, M. Overhand, B. Jaun, D. Rigo, L. Oberer, U. Hommel, R. Amstutz, H. Widmer, *Helv. Chim. Acta* **1996**, *79*, 2043, b) D. Seebach, S. Abele, K. Gademann, G. Guichard, T. Hintermann, B. Jaun, J. L. Matthews, J. V. Schreiber, L. Oberer, U. Hommel, H. Widmer, *Helv. Chim. Acta* **1998**, *81*, 932.

- [26] T. Hintermann, D. Seebach, *Synlett* **1997**, 437.
- [27] G. Guichard, S. Abele, D. Seebach, *Helv. Chim. Acta* **1998**, *81*, 187.
- [28] R. Koradi, M. Billeter, K. Wütrich, *J. Mol. Graph.* **1996**, *14*, 51.
- [29] D. Seebach, K. Gademann, J. V. Schreiber, J. L. Matthews, T. Hintermann, B. Jaun, L. Oberer, U. Hommel, H. Widmer, *Helv. Chim. Acta* **1997**, *80*, 2033, M. Rueping, J. V. Schreiber, G. Lelais, B. Jaun, D. Seebach, *Helv. Chim. Acta* **2002**, *85*, 2577, P. I. Arvidsson, J. Frackenhohl, D. Seebach, *Helv. Chim. Acta* **2003**, *86*, 1522.
- [30] D. Seebach, T. Sifferlin, P. A. Mathieu, A. Häne, C. M. Krell, D. Bierbaum, S. Abele, *Helv. Chim. Acta* **2000**, *83*, 2849, D. Seebach, J. V. Schreiber, P. I. Arvidsson, J. Frackenhohl, *Helv. Chim. Acta* **2001**, *84*, 271, A. Glättli, X. Daura, D. Seebach, W. F. van Gunsteren, *J. Am. Chem. Soc.* **2002**, *124*, 12972, X. Daura, D. Bakowies, D. Seebach, J. Fleischhauer, W. F. van Gunsteren, P. Krüger, *Eur. Biophys. J.* **2003**, *32*, 661.
- [31] K. Gademann, T. Kimmerlin, D. Hoyer, D. Seebach, *J. Med. Chem.* **2001**, *44*, 2460; D. Seebach, M. Rueping, P. I. Arvidsson, T. Kimmerlin, P. Micuch, C. Noti, *Helv. Chim. Acta* **2001**, *84*, 3503; C. Nunn, M. Rueping, D. Langenegger, E. Schuepbach, T. Kimmerlin, P. Micuch, K. Hurth, D. Seebach, D. Hoyer, *Naunyn-Schmiedeberg's Arch Pharmacol.* **2003**, 367, 95.
- [32] D. Seebach, M. Brenner, M. Rueping, B. Jaun, *Chem.–Eur. J.* **2002**, *8*, 573.
- [33] K. Gademann, B. Jaun, D. Seebach, R. Perozzo, L. Scapozza, G. Folkers, *Helv. Chim. Acta* **1999**, *82*, 1.
- [34] T. Etezady-Esfarjani, C. Hilty, K. Wütrich, M. Rueping, J. V. Schreiber, D. Seebach, *Helv. Chim. Acta* **2002**, *85*, 1197.
- [35] X. Daura, W. F. van Gunsteren, D. Rigo, B. Jaun, D. Seebach, *Chem.–Eur. J.* **1997**, *3*, 1410; X. Daura, B. Jaun, D. Seebach, W. F. van Gunsteren, A. E. Mark, *J. Mol. Biol.* **1998**, *280*, 925.
- [36] J. X. Qiu, E. J. Petersson, E. E. Matthews, A. Schepartz, *J. Am. Chem. Soc.* **2006**, *128*, 11338.
- [37] W. S. Hancock, J. E. Battersby, *Anal. Biochem.* **1976**, *71*, 260.
- [38] T. D. Goddard, D. G. Kneller, 'program SPARKY v3.110' University of California, San Francisco, 2004.
- [39] C. D. Schweiters, J. J. Kszewski, N. Tjandra, G. M. Clore, *J. Magn. Reson.* **2003**, *160*, 65.
- [40] E. G. Stein, L. M. Rice, A. T. Brünger, *J. Magn. Reson.* **1997**, *124*, 154.

Received October 18, 2007